Benalia, Sara; Tesfaye, Fiseha; Lindberg, Daniel; Sibarani, David; Hupa, Leena; Chartrand, Patrice; Robelin, Christian

Critical Evaluation and Calorimetric Study of the Thermodynamic Properties of Na_2CrO_4, K_2CrO_4, Na_2MoO_4, K_2MoO_4, Na_2WO_4, and K_2WO_4

Published in:
Journal of Physical and Chemical Reference Data

DOI:
10.1063/5.0154609

Published: 06/12/2023

Document Version
Publisher's PDF, also known as Version of record

Journal of Physical and Chemical Reference Data

RESEARCH ARTICLE | DECEMBER 06 2023

Critical Evaluation and Calorimetric Study of the Thermodynamic Properties of Na_2CrO_4, K_2CrO_4, Na_2MoO_4, K_2MoO_4, Na_2WO_4, and K_2WO_4

Sara Benalia ; Fiseha Tesfaye ; Daniel Lindberg; David Sibarani ; Leena Hupa; Patrice Chartrand; Christian Robelin

J. Phys. Chem. Ref. Data 52, 043102 (2023)
https://doi.org/10.1063/5.0154609

Journal of Physical and Chemical Reference Data ARTICLE pubs.aip.org/aip/jpr

Critical Evaluation and Calorimetric Study of the Thermodynamic Properties of Na_2CrO_4, K_2CrO_4, Na_2MoO_4, K_2MoO_4, Na_2WO_4, and K_2WO_4

Cite as: J. Phys. Chem. Ref. Data 52, 043102 (2023); doi: 10.1063/5.0154609
Submitted: 14 April 2023 • Accepted: 27 October 2023 •
Published Online: 6 December 2023

Sara Benalia,[1,2] Fiseha Tesfaye,[2] Daniel Lindberg,[3] David Sibarani,[3] Leena Hupa,[2] Patrice Chartrand,[1] and Christian Robelin[1,a)]

AFFILIATIONS

[1] Department of Chemical Engineering, Centre for Research in Computational Thermochemistry (CRCT), Polytechnique Montréal, Box 6079, Station Downtown, Montréal, Quebec H3C 3A7, Canada
[2] Laboratory of Molecular Science and Engineering, Johan Gadolin Process Chemistry Centre, Åbo Akademi University, Henrikinkatu 2, FI-20500 Turku, Finland
[3] Department of Chemical and Metallurgical Engineering, School of Chemical Engineering, Aalto University, FI-00076 Aalto, Finland

[a)] **Author to whom correspondence should be addressed:** christian.robelin@polymtl.ca

ABSTRACT

This paper evaluates crystallographic data and thermodynamic properties for sodium chromate, potassium chromate, sodium molybdate, potassium molybdate (K_2MoO_4), sodium tungstate, and potassium tungstate collected from the literature. A thorough literature review was carried out to obtain a good understanding of the available data, and a critical evaluation has been performed from room temperature to above the melting temperatures. Also, the solid–solid transition and melting properties of the six pure salts were measured by differential scanning calorimetry, and high-temperature x-ray powder diffraction measurements were performed to determine the crystal structures and space groups associated with the phases of K_2MoO_4. This work is the first step towards the development of a thermodynamic model for the Na^+, $K^+//Cl^-$, SO_4^{2-}, CO_3^{2-}, CrO_4^{2-}, $Cr_2O_7^{2-}$, MoO_4^{2-}, $Mo_2O_7^{2-}$, WO_4^{2-}, $W_2O_7^{2-}$, O^{2-} system that is relevant for high temperature corrosion in atmospheres containing O–H–S–C–Cl and alkali salts.

CONTENTS

List of Tables

List of Figures

1. Introduction

Combustion installations suffer from the problem of hot corrosion, which limits their efficiency.[1–4] This phenomenon is an accelerated form of oxidation (from 600 to 950 °C)[5,6] affecting equipment in the presence of high-temperature combustion gases (N_2, CO_2, CO, O_2, H_2O, etc.) containing impurities (SO_2, Cl_2, S_2, HCl, etc.) and corrosive products (Na_2O, K_2O, NaOH, KOH, NaCl, KCl, etc.).[3,4,7] The formation of ashes and corrosive gases is mainly due to the elements K, Na, Ca, Mg, Fe, Al, Si, P, S, Cl, C, H, and O.[8,9] Stainless steels containing the alloying elements Ni, Cr, Mo, W, and V are particularly prone to this problem.[2,4,10–12] They are frequently exposed to gaseous species generated during combustion (O_2, CO_2, SO_2, H_2O) or from the evaporation of ashes (KCl, NaCl, Na_2SO_4, K_2SO_4, Na_2CO_3, K_2CO_3).[3,4,6,13]

Oxides formed from these alloying elements, such as Cr_2O_3,[10,14] MoO_3, WO_3, and V_2O_5,[1,10,12] often react with the KCl, NaCl, Na_2SO_4, K_2SO_4, Na_2CO_3, and K_2CO_3 present during the operating conditions of these installations and/or originating from the fuel used. Those along with the quantity of air required for combustion contribute to the oxidation of the alloying elements. The literature reports that, under operating conditions, corrosive deposits in the form of Na_2CrO_4 and K_2CrO_4[14,15] may be formed on the walls of installations. Other salts can further enhance the corrosion, particularly sodium molybdate (Na_2MoO_4),[15,16] potassium molybdate (K_2MoO_4), sodium tungstate (Na_2WO_4),[15,17] and potassium tungstate (K_2WO_4). These may be present in solid or liquid form.

Studies by Misra and Stearns[11] and Fryberg *et al.*[16] revealed the complete conversion of Na_2SO_4 to Na_2CrO_4 before the onset of catastrophic corrosion for Mo-containing superalloys. Initiation of catastrophic corrosion was characterized by the conversion of Na_2CrO_4 to Na_2MoO_4 observed in the MoO_3-rich layer at the scale-metal interface, related to fluxing by the Na_2MoO_4–MoO_3 mixture.

Catastrophic corrosion is attributable to the formation of Na_2MoO_4 and a Na_2MoO_4–MoO_3 mixture, but its mechanisms are still unclear. The presence of sodium in the MoO_3–WO_3 zones reduces the melting temperature by forming Na_2MoO_4–Na_2WO_4.[16] Furthermore, Bourhis and Saint-John[18] reported catastrophic corrosion in Mo-containing superalloys related to fluxing by MoO_3, which forms at the scale-metal interface.

In this context, predicting potential corrosion products to ensure the preservation of equipment while maximizing the rate of conversion into electrical energy is extremely important. Indeed, the various deposits, rich in salts, are generally very corrosive and, when present in liquid form, often dissolve the protective oxide layers and attack the metal surface.[19]

A thermodynamic model for the Na^+, K^+//Cl^-, SO_4^{2-}, CO_3^{2-}, CrO_4^{2-}, $Cr_2O_7^{2-}$, MoO_4^{2-}, $Mo_2O_7^{2-}$, WO_4^{2-}, $W_2O_7^{2-}$, O^{2-} system is being developed. This will permit us to make phase equilibrium calculations, and thus assess the limiting conditions under which deposits are susceptible to form and then prevent their formation. As a first step, it is necessary to investigate the crystal structures and thermodynamic properties (including solid–solid transitions and fusion) of all relevant pure salts. The present article is devoted to a thorough literature review for the sodium and potassium chromates, molybdates, and tungstates. The sodium and potassium dichromates, dimolybdates and ditungstates will be discussed in a subsequent paper. For the six compounds considered in this work, literature data are sometimes lacking or contradictory. Therefore, differential scanning calorimetry (DSC) was used to measure the temperature and enthalpy change for the solid–solid transitions and fusion of the various compounds investigated. In addition, high temperature x-ray diffraction (XRD) measurements were conducted for K_2MoO_4.

2. Experimental Procedure

2.1. DSC/TGA (differential scanning calorimetry/thermogravimetric analysis)

2.1.1. Materials and measurements

The initial reagents used in this study were 99.999% pure Ar (gas) from Oy Linde Gas AB (Finland), $Na_2CrO_4 \cdot 4H_2O$, K_2CrO_4, Na_2MoO_4, K_2MoO_4, $Na_2WO_4 \cdot 2H_2O$, and K_2WO_4. The following Table presents the supplier's name, Chemical Abstracts Service (CAS) number, and purity for each solid reagent.

Chemical formula	Supplier	CAS number	Purity (%)
$Na_2CrO_4 \cdot 4H_2O$	Sigma-Aldrich	10034-82-9	99.0
K_2CrO_4	Alfa-Aesar	7789-00-6	99.9
Na_2MoO_4	Sigma-Aldrich	7631-95-0	99.9
K_2MoO_4	Sigma-Aldrich	13446-49-6	98
$Na_2WO_4 \cdot 2H_2O$	Sigma-Aldrich	10213-10-2	99.995
K_2WO_4	Alfa-Aesar	7790-60-5	99.5

DSC/TGA experiments were conducted to measure the temperature and enthalpy change for the solid–solid transitions and fusion of the pure compounds Na_2CrO_4, K_2CrO_4, Na_2MoO_4, K_2MoO_4, Na_2WO_4, and K_2WO_4. These measurements were performed using a NETZSCH STA 449 F1 Jupiter® simultaneous DSC-TGA equipment.

The calibration of the DSC apparatus was performed using the known enthalpy changes and transition temperatures of the following reference substances (ultra-pure salts):

$$BaCO_3 \ (\text{purity of } 99.98\%) \text{ with } T_{trs}(\text{I} \rightarrow \text{II}) = 808\ ^\circ\text{C};$$

$$CsCl \ (\text{purity of } 99.99\%) \text{ with } T_{trs}(\text{I} \rightarrow \text{II}) = 476\ ^\circ\text{C};$$

$$Ag_2SO_4 \ (\text{purity of } 99.999\%) \text{ with } T_{trs}(\text{I} \rightarrow \text{II}) = 426\ ^\circ\text{C};$$

and

$$C_6H_5COOH \ (\text{purity of } 99.5\%) \text{ with } T_{trs}(\text{sol} \rightarrow \text{L}) = 122\ ^\circ\text{C}.$$

Variations recorded during the calibration measurements were used to estimate the experimental error for the temperatures and enthalpy changes as ±1 °C and ±10% minimum, respectively.

A dehydration treatment of all pure compounds was performed prior to the DSC measurements. This operation was performed in a Vulcan oven temperature (Model: 3-130) to eliminate water

absorbed by the samples during their storage, and also most of the water present in the initial reagents $Na_2CrO_4 \cdot 4H_2O$ and $Na_2WO_4 \cdot 2H_2O$. All reagents were heated for 3 h at 200 °C and then cooled to 25 °C.

About 45 mg of the dehydrated samples were added in a Pt/Rh (80/20) crucible, and a flow rate of 70 ml/min of Ar was used as a protective gas in all runs.

Initial heating was performed from room temperature to 40 °C, followed by a 10 min isothermal hold to ensure thermal stability of the sample and reference. Three consecutive heating–cooling cycles were then conducted for each sample, with a heating/cooling rate of 10 °C/min.

The maximum temperature investigated was always 49 °C above the predetermined melting temperature of each compound while the minimum temperature investigated was at least 50 °C below the temperature of the first solid–solid transition, with a holding time of 1 min in each case. The maximum temperature selected was low enough to avoid vaporization of the compound, but high enough to ensure complete fusion.

Thermogravimetric analysis (TGA) was conducted to monitor mass loss or volatilization. Mass loss and heat flux were both measured continuously throughout the DSC experiments. A maximum mass loss of −3% was always targeted during the experiments. For each pure compound, the overall mass loss was monitored at the end of each DSC experiment: −1.08% for Na_2CrO_4, −1.01% for K_2CrO_4, −0.12% for Na_2MoO_4, −0.1% for K_2MoO_4, −0.02% for Na_2WO_4, and −0.63% for K_2WO_4.

Each solid–solid transition and melting temperature was defined as the temperature at the onset of the peak. The first heating/cooling cycle was always discarded owing to non-reproducible data (i.e., thermal history of the sample).

2.1.2. Setting up the baseline

The first requirement is to establish a baseline before making the actual measurement for a sample. This can be obtained from the signal recorded during a temperature cycle applied to two empty crucibles.

The difference between the baseline and the signal obtained, under the same experimental conditions (i.e., nature of crucibles, temperature profile, heating/cooling rate, and flow rate of gas), depends on the material whose thermal behavior is to be studied. It is essential to have a suitable baseline for each analysis program. Pt/Rh (80/20) crucibles with the same mass were used for the baseline (blank run), the sapphire holder, and the sample holder in all DSC-TGA experiments.

2.2. High temperature x-ray diffraction

XRD patterns for K_2MoO_4 were determined using a 98% purity commercial sample in powder form purchased from Sigma-Aldrich, Germany.

The powder was ground in an agate mortar to ~50 μm particle size to ensure cohesion and then spread evenly on a flat sample holder. The used XRD device was X'Pert Pro MPD Powder model (by Malvern Panalytical), which was connected to a high-temperature chamber Anton Paar HTK 1200N and temperature controller TCU1000N. This setup enabled autonomous temperature control and diffraction measurements. Tube gave CuKα radiation and was set at 40 kV and 40 mA.

The sample holder was equipped with an alumina ring as the sample crucible and Pt–10%Rh thermocouple (type-S) to provide good correspondence between actual and set temperatures. Measurements were carried out at 25, 350, 465, and 500 °C, with a heating rate of 10 °C/min between set points. After the measurement at 500 °C, the sample was cooled to 25 °C and the measurement was repeated at this temperature to confirm the stability of the sample. Measurements were done in a normal air atmosphere and using a secondary monochromator. Measurement angles were from 10° to 70° for a total duration of 1 h per temperature point. The sample was held at a temperature set point for 1 h before being scanned so that it had time to react or change morphology.

3. Crystal Structures and Space Groups

A critical review of the literature related to the crystal structures and space groups of the six pure compounds is provided in this section.

Crystal structure information for phases of Na_2CrO_4 and K_2CrO_4 is summarized in Tables 1 and 2, respectively.

Miller's[20] visual estimation in single-crystal x-ray oscillation intensities showed that Na_2CrO_4(I) (low-temperature phase) is orthorhombic with D^6_{2h}-Pbnn space group. This study was subsequently reviewed by Fischmeister,[21] Niggli,[22] Goldberg *et al.*,[23] Nimmo,[24] and Amirthalingam and Venkateswarlu[25] who confirmed a different space group, Cmcm.

The crystal structure of K_2CrO_4(I) at room temperature has been investigated by XRD.[23,26,27] An orthorhombic structure has been reported with space group Pnam[26,27] or Pcmn.[23]

The high-temperature phases Na_2CrO_4(II) and K_2CrO_4(II) exhibit hexagonal structures. The analysis of high-temperature XRD diffractograms of A_2BX_4-type compounds suggests the space group $P6_3mc$ for both phases with the presence of c-glide;[29] the two structures are isostructural with that of α-Ca_2SiO_4.[23] For Na_2CrO_4(II), Ferrante *et al.*[26] reported the space group P6/mmc. The XRD analysis of Pistorius[27] suggested that K_2CrO_4(II) has the same space group as K_2SO_4: P6/mmc, P6mc, $P\bar{6}2c$, $P\bar{3}1c$, or P31c.

Crystal structure information for phases of Na_2MoO_4 is summarized in Table 3.

The structure of the low-temperature phase (I) of Na_2MoO_4 is a spinel according to Lindqvist *et al.*,[30] with cubic crystal

TABLE 1. Crystallographic data for phases of Na_2CrO_4

Phase	Crystal structure	T (°C)	Space group	Reference
Na_2CrO_4(I)	Orthorhombic	<419	D^6_{2h}-Pbnn	20
				21
			Cmcm	22
				23
				24
				25
Na_2CrO_4(II)	Hexagonal	419–793	$P6_3mc$	23
			$P6_3/mmc$	26

TABLE 2. Crystallographic data for phases of K_2CrO_4

Phase	Crystal structure	T (°C)	Space group	Reference
K_2CrO_4(I)	Orthorhombic	<669	Pcmn	23
			Pnam	27
			···	28
K_2CrO_4(II)	Hexagonal	669–976	$P6_3mc$	23
			P6/mmc, P6mc, $P\bar{6}2c$, $P\bar{3}1c$, P31c	27

TABLE 3. Crystallographic data for phases of Na_2MoO_4

Phase	Crystal structure	T (°C)	Space group	Reference
Na_2MoO_4(I)	Cubic	<458	···	30
			Fd3m	31
			···	32
				33
			$Fd\bar{3}m$	34
				35
Na_2MoO_4(II)	Orthorhombic	458–592	···	32
			$Pbn2_1$	Reference 10 in Ref. 36
Na_2MoO_4(III)	Orthorhombic	592–641	···	32
			Fddd	Reference 10 in Ref. 36
				34
Na_2MoO_4(IV)	Hexagonal	641–687	$P6_3/mmc$	Reference 10 in Ref. 36
				34
			···	32

structure.[30–35] XRD revealed the $Fd\bar{3}m$ space group,[34] and further studies by Raman spectroscopy[33] and neutron powder diffraction[35] yielded the same space group. Swanson[31] reported the Fd3m space group. XRD patterns showed that the second phase (II) of Na_2MoO_4 is orthorhombic[32,36] with space group $Pbn2_1$.[36] The transition from II to III yielded the same crystal structure[32,34,36] with the Fddd space group.[34,36] The high-temperature phase IV is hexagonal[32,34,36] with space group $P6_3/mmc$.[34,36]

Crystal structure information for phases of K_2MoO_4 is summarized in Table 4.

K_2MoO_4 exhibits three phases. The low-temperature form I is monoclinic. Our XRD analysis, the measurements of Ref. 37 (who performed three-dimensional Patterson and Fourier syntheses that were refined by least squares techniques) and those of Refs. 38–40 confirmed C2/m as the space group.

Our high-temperature XRD analysis showed that II is orthorhombic, in agreement with Refs. 40 and 41. The space group identified by us (Ccmm) agrees with that reported by Van Den Berg *et al.*[41]

III has also been studied by us using high-temperature XRD up to 500 °C; analysis of the diffractogram indicated a trigonal structure. Van Den Akker *et al.*[42] erroneously reported an hexagonal structure. According to our results, the space group is $P\bar{3}m1$, in agreement with Van Den Akker *et al.*[42]

According to Warczewski,[39] the transition from the intermediate-temperature phase II to the high-temperature pseudohexagonal phase III involves two modulated intermediate structures (incommensurable), which are orthorhombic and

TABLE 4. Crystallographic data for phases of K_2MoO_4

Phase	Crystal structure	T (°C)	Space group	Reference
K_2MoO_4(I)	Monoclinic	<324		This work
			C2/m	37
				38
			···	39
			C2/m	40
K_2MoO_4(II)	Orthorhombic	324–455	Ccmm	This work
			···	39
			Ccmm	41
K_2MoO_4(III)	Trigonal	455–928	$P\bar{3}m1$	This work
			···	39
			$P\bar{3}m1$	42

pseudohexagonal, respectively. Based on these data, K_2MoO_4 exhibits four phases, and the high-temperature form (IV) is hexagonal. However, as will be explained later, this fourth phase was not observed in our high-temperature XRD analysis (at 465 and 500 °C). Therefore, only three phases were considered for K_2MoO_4 in the present work.

Crystal structure information for phases of Na_2WO_4 is summarized in Table 5.

There are some uncertainties in the literature regarding the number of phases for Na_2WO_4, as well as their crystal structures and space groups.[33,36,43,46–48] XRD analyses conducted by Pistorius[43] and Temperature-Programmed x-ray powder Diffraction (TPXRD) by Hämmer and Höppe[45] suggested the presence of three phases. However, the XRD analyses performed by Pistorius[43] have only identified with certainty two phases (I and III). For Na_2WO_4(II), the diffraction pattern was of rather poor quality.

XRD analysis,[49] Raman spectroscopy[33] and neutron diffraction[35] confirmed that the low-temperature phase Na_2WO_4(I) is cubic with $Fd\bar{3}m$ space group. At room temperature, only Na_2MoO_4 and Na_2WO_4 exhibit an ordinary spinel structure among alkali metal sulfates, chromates, molybdates and tungstates.[30,35] The work of Hämmer and Höppe[45] was the only one able to characterize the phase II using TPXRD; Austin and Pierce[47] had indicated that both solid–solid transitions were displaced and non-reconstructive. Therefore, obtaining single crystals of the high-temperature phases of Na_2WO_4 by quenching was impossible, as well as the use of Rietveld refinement and DSC. Based on TPXRD data, it is suggested that Na_2WO_4(II) has a tetragonal unit cell with lattice parameters a = 1707.2 pm, c = 1293.6 pm, and a space group consistent with symmetry relationships to Na_2WO_4(I), i.e., I41/amd.[45] The latter is assumed to be a maximal subgroup of $Fd\bar{3}m$ and a direct supergroup of Fddd (space group of the phase III).[45] Even with indexing and Pawley fitting (R_{Bragg} = 0.013, R_{wp} = 0.058), the structure of II was not reliably determined. Thus, Na_2WO_4(II) was assumed to crystallize in the I41/amd space group, with no symmetry relationship derivable between Na_2WO_4(I) and Na_2WO_4(III), and no proposed unit cell fitting into such a structure.[45] Very limited high-temperature XRD studies have been conducted to identify the structure and space group of the phase III; Pistorius[43] and Hämmer and Höppe[45] reported an orthorhombic structure with different space groups (Pnam and Fddd, respectively).

Crystal structure information for phases of K_2WO_4 is summarized in Table 6.

K_2WO_4 displays three phases. The crystal structure was studied at room temperature by Raman spectroscopy[50] and XRD,[39,42] and was found to be monoclinic with C2/m space group.[42] The phase II was examined by XRD only by Van Den Akker *et al.*,[42] who suggested a β-K_2SO_4 type structure. However, the structure has not been reliably identified, and these authors indicated that most potassium salt phases have an orthorhombic structure (β-K_2SO_4 type).

For the phase III, the XRD analyses of Warczewski[39] and Van Den Akker *et al.*[42] revealed a trigonal structure with $P\bar{3}m1$ space group.[42] Note that Refs. 39 and 42 incorrectly reported a hexagonal structure.

TABLE 5. Crystallographic data for phases of Na_2WO_4

Phase	Crystal structure	T (°C)	Space group	Reference
Na_2WO_4(I)	Cubic	<588	Fd3m $Fd\bar{3}m$	43 44 33 35 45
Na_2WO_4(II)	Tetragonal (tentative)	588–589	I41/amd (tentative)	45
Na_2WO_4(III)	Orthorhombic	589–694	Pnam–D_{2h}^{16} Fddd	43 45

TABLE 6. Crystallographic data for phases of K_2WO_4

Phase	Crystal structure	T (°C)	Space group	Reference
K_2WO_4(I)	Monoclinic	<364	... C2/m ...	50 42 39
K_2WO_4(II)	Orthorhombic (β-K_2SO_4 type)	364–458	...	42
K_2WO_4(III)	Trigonal	458–927	$P\bar{3}m1$ ...	42 39

4. Selected Thermodynamic Properties for Na_2CrO_4, K_2CrO_4, Na_2MoO_4, K_2MoO_4, Na_2WO_4, and K_2WO_4

4.1. Sodium chromate

4.1.1. Transition temperature (T_{trs}) and enthalpy change (ΔH_{trs}) of solid–solid transition (I → II) for Na_2CrO_4

To measure the temperature and enthalpy change for the solid–solid transition of Na_2CrO_4, DSC measurements were conducted in this work. In addition, data acquired by various experimental techniques were collected from the literature and are shown in Table 7.

4.1.2. Temperature (T_{fus}) and enthalpy of fusion (ΔH_{fus}) for Na_2CrO_4

The thermodynamic properties of fusion (temperature and enthalpy change) were measured by Refs. 26, 51, 53, 54, and 56–64. The heat of fusion was obtained by drop calorimetry[26,54] and DTA.[53] In this work, DSC measurements were conducted. As an example, the DSC thermogram (second and third heating/cooling cycles only) for Na_2CrO_4 is shown in Fig. 1. The DSC thermograms for all other compounds are presented in the supplementary material. All data collected from the literature and obtained in the present work are presented in Table 8.

4.1.3. Recommended thermodynamic data for sodium chromate Na_2CrO_4

Our selected thermodynamic data ($\Delta_f H^\circ_{298}$, S°_{298}, and C_P) for sodium chromate (Na_2CrO_4) are provided in Table 9. For the pure liquid, below the temperature of fusion, the heat capacity (as a function of temperature) over a given temperature range was taken identical to that of the solid phase stable over this specific temperature range (i.e., C_P of the low-temperature phase I between 298.15

TABLE 7. Transition temperature and enthalpy change of solid–solid transition for Na_2CrO_4

T_{trs} (I → II) (°C)	ΔH_{trs}(I → II) (kJ mol^{-1})	Experimental method	Reference
417.3	8.49[a]	DSC (second heating) at 10 °C/min	This work
417.6	8.27[a]	DSC (third heating) at 10 °C/min	This work
413[a]	···	Cooling curves	51
421 ± 4	···	DTA[b]	52
420	10.04	DTA	53
420.9 ± 3	9.58 ± 0.42	Ice calorimetry, drop method	54
419	8.87[a]	DTA	23
427[a]	9.47	Calorimetry, drop method	26
419.4	10.06 (cooling) 9.60 (heating)	DSC at 10 °C/min	55
419.1 ± 2.7	9.6 ± 0.6	Weighted average	This work

[a]Outlier.
[b]The purity of salt is 99.5%.

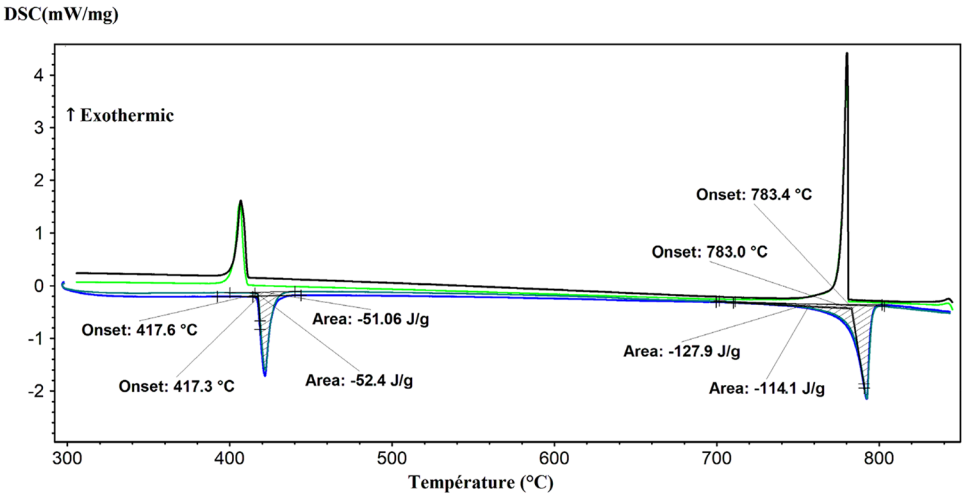

FIG. 1. DSC thermogram for Na_2CrO_4 (second and third heating/cooling cycles only). Blue: second heating, dark green: third heating, light green: second cooling, black: third cooling.

TABLE 8. Transition temperature and enthalpy of fusion for Na_2CrO_4

T_{fus} (II → L) (°C)	ΔH_{fus} (II → L) (kJ mol^{-1})	Experimental method	Reference
783[a]	18.48[a]	DSC (second heating) at 10 °C/min	This work
783.4[a]	19.60[a]	DSC (third heating) at 10 °C/min	This work
792	···	Cooling curves	51
780[a]	···	Pt/Pt–Rh thermocouple; visual	56
794.5	···	Cooling curves	57
792	···	Calibrated TC; recorder potentiometer	58
791.9	···	DTA	59
793	···	Pt/Pt–Rh thermocouple; visual	60
796	25.15	DTA	53
792.4 ± 1	···	DTA; high-T microscopy	61
794	···	Visual-polythermal method	62
796.9 ± 2	24.23 ± 0.42	Ice calorimetry, drop method	54
792	24.31	Calorimetry[b], drop method	26
785.6[a]	···	DTA	63
795.1	···	DTA	64
793.3 ± 3.2	24.3 ± 0.9	Weighted average	This work

[a]Outlier.
[b]The standard error is 0.07% for the determination, and the absolute uncertainty of the enthalpy is estimated to be ±0.3%.

TABLE 9. Selected thermodynamic properties of Na_2CrO_4

Phase	T range (K)	$\Delta_f H^\circ_{298}$ (kJ mol^{-1})[a]	S°_{298} (J mol^{-1} K^{-1})[b]	C_P (J mol^{-1} K^{-1})	Reference
Na_2CrO_4(I)	298.15	−1341.49			This work
			176.62		26
	298.15–692.3			101.07 + 0.139 99T/K	54
Na_2CrO_4(II)	298.15	−1331.86	190.52		This work
	298.15–692.3			101.07 + 0.139 99T/K	54
	692.3–1066.4			149.94 + 0.051 59T/K	54
Na_2CrO_4(L)	298.15	−1307.53	213.34		This work
	298.15–692.3			101.07 + 0.139 99T/K	
	692.3–1066.4			149.94 + 0.051 59T/K	54
	1066.4–2000			204.78	

[a]Enthalpy relative to the enthalpy of the elements in their stable standard states at 298.15 K.
[b]Absolute (third law) entropy.

and 692.3 K, and C_P of the high-temperature phase II between 692.3 and 1066.4 K). Similarly, for solid II, below the temperature of the solid–solid transition, the heat capacity was taken identical to that of solid I. For all three phases, the heat capacity above the maximum temperature T_{max} of the highest temperature range in Table 9 is assumed to be constant and equal to the value of C_P at T_{max}.

The same approach was used for all other compounds considered in this work, even when there were more than two solid phases. More details on the thermodynamic properties selected for Na_2CrO_4 are given below.

The available measurements for the temperature and enthalpy change of the (I → II) and (II → L) transitions for Na_2CrO_4 are shown in Tables 7 and 8, respectively. For each property, the measured values were plotted as a function of the experiment number in order to identify visually outliers (see Figures S6–S9 in the supplementary material). A weighted average was then calculated from the retained measurements, with a weighting based on the expected accuracy of each experimental technique. The weighting factors used for the temperature and enthalpy change are given in Tables S3 and S4, respectively, in the supplementary material. The standard deviation σ was then calculated.

The outliers are identified by the letter "a" in Tables 7 and 8 and are shown in red color in Tables S1 and S2 in the supplementary material, and as empty circles in Figs. S6–S9 in the supplementary material. In these scatter plots, the weighted average is shown as a solid line while the two dashed lines correspond to (weighted

average ±2σ). It was checked that all outliers lie outside this range. The reported uncertainties in Tables 7 and 8 correspond to ±2σ. A similar approach was used for all other compounds investigated in this work.

The value of the standard enthalpy at 298.15 K ($\Delta_f H^\circ_{298}$) for Na_2CrO_4(I) was estimated as follows. The enthalpy of dissolution in water of Na_2CrO_4(I) ($Na_2CrO_{4(I)} \rightarrow 2Na^+_{(aq)} + CrO^{2-}_{4(aq)}$) was measured by calorimetry[65] as −19.12 kJ mol^{-1}. According to the most recent databases of the FactSage software package,[66] $\Delta_f H^\circ_{298}(Na^+_{(aq)})$ = −239.73 kJ mol^{-1} and $\Delta_f H^\circ_{298}(CrO^{2-}_{4(aq)})$ = −881.15 kJ mol^{-1}. The obtained value of −1341.49 kJ mol^{-1} for $\Delta_f H^\circ_{298}$ [Na_2CrO_4(I)] is very close to that of −1342.20 kJ mol^{-1} recommended in Barin's compilation.[67] The Open Quantum Materials Database (OQMD)[68,69] reported an enthalpy of formation at 0 K of −1331.21 kJ mol^{-1} derived from Density Functional Theory (DFT) calculations. The corresponding value given in Materials Project[70] is −1343.37 kJ mol^{-1}.

The standard entropy at 298.15 K (S°_{298}) of Na_2CrO_4(I) was derived by Ferrante *et al.*[26] as 176.62 J mol^{-1} K^{-1} by integration of their experimental C_P values from 5.5 to 308.5 K using adiabatic calorimetry. This value is identical to that recommended in Barin's compilation (176.61 J mol^{-1} K^{-1}).[67]

To our knowledge, no other direct heat capacity measurements are available for Na_2CrO_4. Denielou *et al.*[54] carried out heat content measurements using drop calorimetry in an ice calorimeter. The salts were then analyzed using XRD to confirm that they were in their stable form. Enthalpy variations $H_T - H_{273}$ as a function of temperature were obtained as follows. For $Na_2CrO_{4(I)}$, 9 measurements were performed between 370 and 665 K, and the following fit was provided by Denielou *et al.*:[54] $H_T - H_{273}$ = 6.999 × 10^{-5} T^2 + 10.107 × 10^{-2}T − 32.78 kJ mol^{-1} (0.4%, empirical standard deviation of 0.03 kJ).[54] For Na_2CrO_4(II), 11 measurements were conducted between 698 and 1065 K, with the following fit: $H_T - H_{273}$ = 2.580 × 10^{-5} T^2 + 14.994 × 10^{-2}T − 35.84 kJ mol^{-1} (0.15%, empirical standard deviation of 0.03 kJ).[54] Finally, for Na_2CrO_4(L), at least 11 measurements were made above 1091 K, with the following fit: $H_T - H_{273}$ = 20.478 × 10^{-2} T − 40.74 kJ mol^{-1} (0.11%, empirical standard deviation of 0.05 kJ).[54]

For each phase of Na_2CrO_4, the heat capacity expression (as a function of temperature) was derived by us from the fits of $H_T - H_{273}$ provided by Denielou *et al.*[54] Calculated values of $H_T - H_{298}$ are compared to the available data in Fig. 2. This figure includes the heat contents $H_T - H_{298}$ measured by Ferrante *et al.*[26] as well as the $H_T - H_{298}$ values obtained by conversion of the $H_T - H_{273}$ data of Denielou *et al.*[54] [$H_T - H_{298}$ = ($H_T - H_{273}$) − ($H_{298} - H_{273}$)]. These two series of data are in good agreement.

4.2. Potassium chromate

4.2.1. Transition temperature (T_{trs}) and enthalpy change (ΔH_{trs}) of solid–solid transition (I → II) for K_2CrO_4

The temperature and enthalpy change for the solid–solid transition of K_2CrO_4 was measured by DSC in the present work. These data along with all measurements collected from the literature (and obtained using various experimental techniques) are gathered in Table 10. Our experimental DSC thermogram is provided in the supplementary material (Fig. S1).

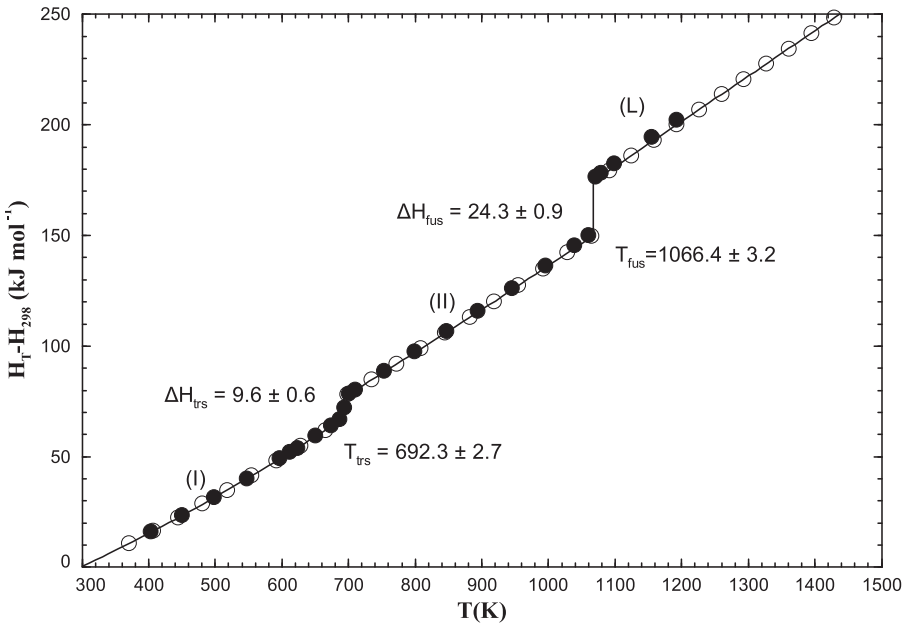

FIG. 2. Calculated heat content $H_T - H_{298}$ for Na_2CrO_4 (enthalpies of transition are the weighted average of all available data presented in Tables 7 and 8). Experimental data from Refs. 26 (●) and 54 (○).

TABLE 10. Transition temperature and enthalpy change of solid–solid transition for K_2CrO_4

T_{trs} (I → II) (°C)	ΔH_{trs}(I → II) (kJ mol^{-1})	Experimental method	Reference
670.7	7.201	DSC (second heating) at 10 °C/min	This work
671.2	7.123	DSC (third heating) at 10 °C/min	This work
666	···	Heating or cooling curves	71
679[a]	···	Pyrometry	72
669	···	Cooling curves	51
666	···	Cooling curves; visual	73
664	10.251[a]	Heating or cooling curves	74
666.8	···	Thermocouple Pt–Rh	75
669	···	Cooling curves	76
663	···	Resistance technique	27
671	7.155	DTA	53
665	10.2[a]	···	77
668.5 ± 3	···	DTA[b]	78
675	···	DTA[c]	79
662.9 ± 3	9.954 ± 0.502[a]	Ice calorimeter, enthalpimetry	80
674	6.583 5.243[a]	DSC[d] at 5 °C/min DTA[d] at 5 °C/min	81
	7.2 ± 0.25	DSC	
670.2 ± 3	6.908[e]	10 °C/min (heating) 40 °C/min (cooling)	82
668.9	···	Elect conduct (single crystal)	83
669.2 ± 7.1	7.0 ± 0.5	Weighted average	This work

[a]Outlier.
[b]The purity of this salt is 99.8%.
[c]The purity of this salt is 99.96%.
[d]The purity of this salt is 99.87%.
[e]Questionable according to the authors.

4.2.2. Temperature (T_f) and enthalpy of fusion (ΔH_f) for K_2CrO_4

The temperature and enthalpy of fusion have been measured by Refs. 51, 53, 59, 61, 71–73, 75, 77, 80, and 84–88. The heat of fusion was obtained by enthalpimetric analysis[80] and DTA.[53] All data from the literature and our DSC measurements are given in Table 11.

4.2.3. Recommended thermodynamic data for potassium chromate K_2CrO_4

Our selected thermodynamic data ($\Delta_f H^\circ_{298}$, S°_{298}, and C_P) for potassium chromate (K_2CrO_4) are given in Table 12.

The standard enthalpy at 298.15 K of −1403.70 kJ mol^{-1} for K_2CrO_4(I) was taken directly from the National Bureau of Standards (NBS) Tables of chemical thermodynamic properties of Wagman *et al.*,[89] since no experimental values were found in the literature. OQMD[68,69] reported an enthalpy of formation at 0 K of −1362.95 kJ mol^{-1} using DFT calculations. The corresponding value given in Materials Project[70] is −1394.70 kJ mol^{-1}.

The standard entropy at 298.15 K (S°_{298}) reported by Popov and Kolesov[90] (see Table 12) is in very good agreement with that in the book edited by Lax[77] (i.e., 200 J mol^{-1} K^{-1}), and also with that from Barin[67] (i.e., 199.99 J mol^{-1} K^{-1}). The value from Popov and Kolesov is the only experimental value found in the literature; it was obtained by integration of $\int_{0K}^{298.15K} \frac{C_P}{T} dT$, where the low-temperature heat capacity was measured by calorimetry.

To our knowledge, there are no other direct C_P measurements for K_2CrO_4 available in the literature. Heat content ($H_T - H_{298}$) measurements were conducted by Sirousse-Zia[80] using 99.5% certified material and enthalpimetric analysis in an ice calorimeter. This author obtained 11 experimental values for each phase ($K_2CrO_{4(I)}$, $K_2CrO_{4(II)}$, and $K_2CrO_{4(L)}$), and derived a fit of $H_T - H_{298}$ as a function of temperature. For I, between 517 and 888 K, $H_T - H_{298} = 3.622 \times 10^{-8} T^3 - 2.227 \times 10^{-5} T^2 + 16.336 \times 10^{-2} T - 45.89$ kJ mol^{-1} (0.7%, empirical standard deviation of 0.06 kJ). The corresponding value is 1.776 kJ mol^{-1} at 298.15 K. The following new fit, which is null at 298.15 K, was obtained by us: $3.059\,523 \times 10^{-5} (T - 298.15)^2 + 1.625\,099 \times 10^{-1} (T - 298.15)$ kJ mol^{-1}.

Sirousse-Zia[80] also derived the following fits: for II, between 942 and 1202 K, $H_T - H_{298} = 7.669 \times 10^{-5} T^2 + 4.489 \times 10^{-2} T + 17.95$ kJ mol^{-1} (0.4%, empirical standard deviation of 0.05 kJ); for the pure liquid, above 1261 K, $H_T - H_{298} = 2.120 \times 10^{-1} T - 38.17$ kJ mol^{-1} (0.4%, empirical standard deviation of 0.05 kJ). For each phase of K_2CrO_4, the heat capacity expression (as a function of temperature) was derived (see Table 12) from the fits of $H_T - H_{298}$ given previously. Calculated values of $H_T - H_{298}$ are shown along with the available data in Fig. 3. Our calculations somewhat underestimate the measurements of Sirousse-Zia[80] for the high-temperature phase and the pure liquid since the selected

TABLE 11. Transition temperature and enthalpy of fusion for K_2CrO_4

T_{fus} (II → L) (°C)	ΔH_{fus} (II → L) (kJ mol^{-1})	Experimental method	Reference
977.2	32.896	DSC (second heating) at 10 °C/min	This work
976.4	34.197	DSC (third heating) at 10 °C/min	This work
971	···	Heating or cooling curves	71
984	···	Pyrometry	72
976	···	Cooling curves	51
978	···	Cooling curves; visual	73
968.3	···	Thermocouple Pt–Rh	75
970.9	···	Cooling curves	84
976	···	DTA	59
972	···	Visual-polythermal method	85
979	31.547	DTA	53
984	28.9[a]	···	77
980	···	DTA and high-temperature microscopy	61
984	···	DTA	86
976	···	Visual-polythermal method	87
968	···	Pt/Pt–Rh thermocouple; visual	88
973.9 ± 4	32.991 ± 0.669	Ice calorimeter, enthalpimetry	80
975.9 ± 9.9	33.1 ± 1.8	Weighted average	This work

[a]Outlier.

TABLE 12. Selected thermodynamic properties of K_2CrO_4

Phase	T range (K)	$\Delta_f H^\circ_{298}$ (kJ mol^{-1})	S°_{298} (J mol^{-1} K^{-1})	C_P (J mol^{-1} K^{-1})	Reference
K_2CrO_4(I)	298.15	−1403.70	199.99		89
					90
	298.15–942.4			144.28 + 0.061 19T/K	80
K_2CrO_4(II)	298.15	−1396.66	207.47		This work
	298.15–942.4			144.28 + 0.061 19T/K	
	942.4–1249.1			44.89 + 0.153 39T/K	80
	1249.1–2000[a]			212.01	
K_2CrO_4(L)	298.15	−1363.55	233.97		This work
	298.15–942.4			144.28 + 0.061 19T/K	
	942.4–1249.1			44.89 + 0.153 39T/K	80
	1249.1–2000			212.01	

[a]Above the temperature of fusion, the heat capacity of K_2CrO_4(II) was assumed to be equal to that of K_2CrO_4(L) to ensure a reasonable extrapolation of the Gibbs energy at high temperatures. In absence of this additional C_P range, the high-temperature phase would be calculated to be more stable than the pure liquid above 6814 K.

enthalpy changes for the solid–solid transition and the fusion are weighted averages of all available data from the literature and of our own DSC measurements.

4.3. Sodium molybdate

4.3.1. Transition temperature (T_{trs}) and enthalpy change (ΔH_{trs}) of solid-solid transitions (I → II, II → III, and III → IV) for Na_2MoO_4

The temperatures and enthalpy changes for the various solid–solid transitions (I → II, II → III, and III → IV) of Na_2MoO_4 were measured by DSC in this work. These data along with all measurements available in the literature are shown in Tables 13–15, respectively. Our experimental DSC thermogram is presented in the supplementary material (Fig. S2).

4.3.2. Temperature (T_{fus}) and enthalpy of fusion (ΔH_{fus}) for Na_2MoO_4

The properties of fusion (temperature and enthalpy change) were measured by Refs. 32, 36, 53, 54, and 91–97. The enthalpy of fusion was obtained using DTA,[53] drop calorimetry,[54] calorimetry,[94] and DSC.[93] All data collected from the literature and our own DSC measurements are displayed in Table 16.

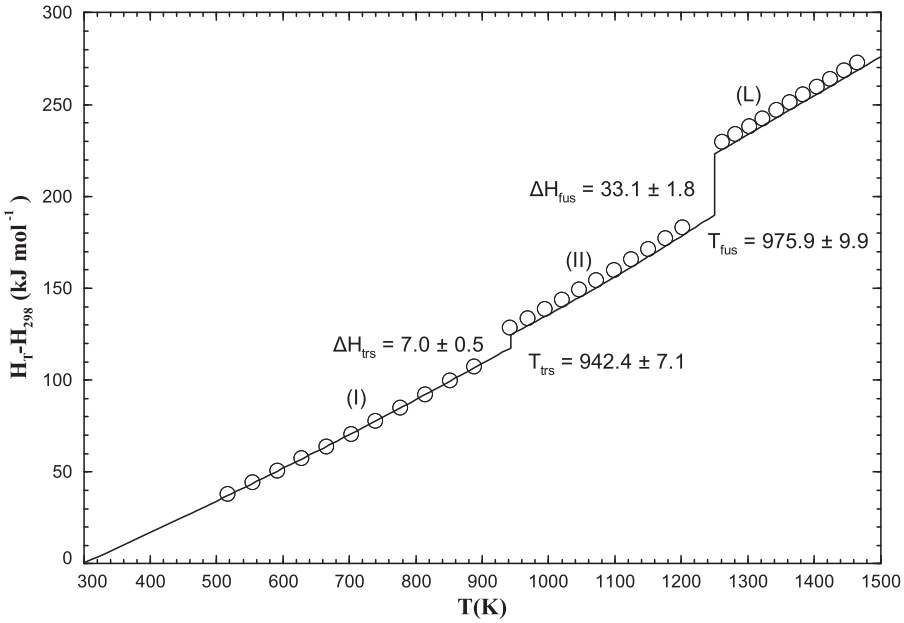

FIG. 3. Calculated heat content $H_T - H_{298}$ for K_2CrO_4 (enthalpies of transition are the weighted average of all available data presented in Tables 10 and 11). Experimental data from Ref. 80 (○).

TABLE 13. Transition temperature and enthalpy change of transition I → II for Na_2MoO_4

T_{trs} (I → II) (°C)	ΔH_{trs} (I → II) (kJ mol^{-1})	Experimental method	Reference
455.8	22.447	DSC (second heating) at 10 °C/min	This work
456.7	22.097	DSC (third heating) at 10 °C/min	This work
440[a]	61.086[a]	Heating or cooling curves	74
457.9 ± 2	26.65	DTA	53
454.9 ± 1	···	DTA at 5 °C/min	91
444.9 ± 2[a]	21.76 ± 0.38	Calorimetry, drop method	54
460.9	···	DSC (cooling) at 3 °C/min	36
440.9 (run 1)[a]	···		
435.9 (run 2)[a]	···	DTA (1.8 and 10.2 °C/min)	92
441.9 (run 3)[a]	···		
459.9	···	DTA (heating) at 10 °C/min	32
457.85	···	DSC at 10 °C/min	
509.9–529.9[a]	···	Raman spectroscopy	33
456.9 ± 1	26.78 ± 0.38	DSC at (10, 5 and 2 °C/min)	93
457.6 ± 3.7	23.1 ± 4.9	Weighted average	This work

[a]Outlier.

4.3.3. Recommended thermodynamic data for sodium molybdate Na_2MoO_4

Our selected thermodynamic data ($\Delta_f H^\circ_{298}$, S°_{298}, and C_P) for sodium molybdate (Na_2MoO_4) are shown in Table 17.

The molar enthalpy of dissolution of Na_2MoO_4 in a NaOH solution was measured at 298.15 K by Tangri *et al.* using an isoperibol calorimeter.[98] The molar enthalpy of solution at infinite dilution was measured as −11.79 ± 0.51 kJ mol^{-1},[98] and a standard enthalpy at 298.15 K of −1465.87 kJ mol^{-1} was then derived for Na_2MoO_4(I). Using a cycle of calorimetric reactions, Koehler *et al.*[100] evaluated $\Delta_f H^\circ_{298}$ = −1467.75 kJ mol^{-1}. The value recommended in Barin's compilation tables[67] is −1469.00 kJ mol^{-1}. The $\Delta_f H^\circ_{298}$ value reported by Tangri *et al.*[98] was selected in the present work. OQMD[68,69] reported an enthalpy of formation at 0 K of −1560.17 kJ mol^{-1} using DFT. The corresponding value given in Materials Project[70] is −1456.16 kJ mol^{-1}.

TABLE 14. Transition temperature and enthalpy change of transition II → III for Na_2MoO_4

T_{trs} (II → III) (°C)	ΔH_{trs} (II → III) (kJ mol^{-1})	Experimental method	Reference
591.4	1.685	DSC (second heating) at 10 °C/min	This work
591.4	1.700	DSC (third heating) at 10 °C/min	This work
590.9 ± 2	1.88	DTA	53
579.9 ± 2[a]	···	DTA at 5 °C/min	91
592.9 ± 3	2.09 ± 0.38	Calorimetry, drop method	54
591.9	···	DSC (cooling) at 3 °C/min	36
571.9 (run 1)[a]	···		
574.9 (run 2)[a]	···	DTA (1.8 and 10.2 °C/min)	92
569.9 (run 3)[a]	···		
579.9[a]	···	DTA (heating) at 10 °C/min	32
591.9	···	DSC at 10 °C/min	
549.9–639.9	···	Raman spectroscopy	33
592.9 ± 1	2.01 ± 0.33	DSC at (10, 5 and 2 °C/min)	93
591.8 ± 2.5	1.9 ± 0.3	Weighted average	This work

[a]Outlier.

TABLE 15. Transition temperature and enthalpy change of transition III → IV for Na_2MoO_4

T_{trs} (III → IV) (°C)	ΔH_{trs}(III → IV) (kJ mol^{-1})	Experimental method	Reference
642.4	8.316	DSC (second heating) at 10 °C/min	This work
642.4	8.248	DSC (third heating) at 10 °C/min	This work
641.9 ± 2	10.84[a]	DTA	53
637.9 ± 2	···	DTA at 5 °C/min	91
641.9 ± 2	8.28 ± 0.46	Calorimetry, drop method	54
639.9	···	DSC (cooling) at 3 °C/min	36
641.9 ± 2	8.3 ± 0.4	Calorimetry; spectroscopy	94
622.9 (run 1)[a]	···		
625.9 (run 2)[a]	···	DTA (1.8 and 10.2 °C/min)	92
618.9 (run 3)[a]	···		
641.85	···	DTA (heating) at 10 °C/min	32
637.9	···	DSC at 10 °C/min	
669.9–676.9[a]	···	Raman spectroscopy	33
639.9 ± 1	7.81 ± 1.25	DSC at (10, 5 and 2 °C/min)	93
640.6 ± 3.4	8.2 ± 0.4	Weighted average	This work

[a]Outlier.

For the standard entropy at 298.15 K (S°_{298}), Welle and King[99] reported a value of 159.41 J mol^{-1} K^{-1}, estimated by integration of their low-temperature heat capacity measurements obtained by calorimetry. The Einstein and Debye functions were used over the extrapolated temperature range of 0–51 K.

Using adiabatic calorimetry, Gavrichev *et al.*[101] performed low-temperature C_P measurements from 14 to 297 K, and derived a S°_{298} value of 149.9 ± 0.2 J mol^{-1} K^{-1}.

Finally, the S°_{298} value obtained by Weller and King,[99] which is close to the value of 159.41 J mol^{-1} K^{-1} recommended in Barin's compilation tables,[67] was selected in this work.

Using drop calorimetry in an ice calorimeter, Denielou *et al.*[54] performed heat content measurements ($H_T - H_{273}$) for Na_2MoO_4, and derived fits of their data along with C_P expressions (as a function of temperature). The stability of the salts was verified by XRD analyses.

For Na_2MoO_4(I), based on 11 measurements between 427 and 709 K, $H_T - H_{273} = 3.929 \times 10^{-5} T^2 + 1.253 \times 10^{-1} T - 376.02$ kJ mol^{-1} (0.3%, empirical standard deviation of 0.02 kJ). This fit was assumed to be valid from 298.15 K to our selected temperature of 730.7 K for the I → II transition.

Extrapolation to 296.5 K of the heat capacity expression C_P(I) = 0.078 58T + 125.344 27 J mol^{-1} K^{-1} (valid from 427 to 709 K) given by Denielou *et al.*[54] gives a value of 148.64 J mol^{-1} K^{-1}, which agrees well with the heat capacity measurement of Weller and King.[99] Gavrichev *et al.*[101] measured at 298.15 K a value of 131.81 J mol^{-1} K^{-1}, which is about 17 J mol^{-1} K^{-1} lower.

TABLE 16. Transition temperature and enthalpy of fusion for Na_2MoO_4

T_{fus} (IV → L) (°C)	ΔH_{fus} (IV → L) (kJ mol^{-1})	Experimental method	Reference
688.2	18.637	DSC (second heating) at 10 °C/min	This work
686.9	18.495	DSC (third heating) at 10 °C/min	This work
688	···	Visual-polythermal method	95
690	···	DTA	96
692.9 ± 2[a]	24.43[a]	DTA	53
686.9 ± 1	···	DTA at 5 °C/min	91
688.9 ± 3	21.42 ± 0.5	Calorimetry, drop method	54
688.9	···	DSC (cooling) at 3 °C/min	36
685.9 ± 2	20.4 ± 0.4	Calorimetry; spectroscopy	94
687	···	Thermal analysis	97
671.9 (run 1)[a]	···		
674.9 (run 2)[a]	···	DTA (1.8 and 10.2 °C/min)	92
667.9 (run 3)[a]	···		
679.9[a]	···	DSC at 10 °C/min	32
684.9	···	DTA at 10 °C/min	
683.9 ± 1	20.73 ± 1.14	DSC at (10, 5 and 2 °C/min)	93
687.1 ± 3.5	20.4 ± 2.5	Weighted average	This work

[a]Outlier.

TABLE 17. Selected thermodynamic properties of Na_2MoO_4

Phase	T range (K)	$\Delta_f H^\circ_{298}$ (kJ mol^{-1})	S°_{298} (J mol^{-1} K^{-1})	C_P (J mol^{-1} K^{-1})	Reference
Na_2MoO_4(I)	298.15	−1465.87	159.41		98 99
	298.15–730.7			125.34 + 0.078 58T/K	54
Na_2MoO_4(II)	298.15	−1442.80	190.98		This work
	298.15–730.7			125.34 + 0.078 58T/K	54
	730.7–865			−215.46 + 0.506 43T/K	
Na_2MoO_4(III)	298.15	−1440.86	193.22		This work
	298.15–730.7			125.34 + 0.078 58T/K	54
	730.7–865			−215.46 + 0.506 43T/K	
	865–913.7			202.30	This work
Na_2MoO_4(IV)	298.15	−1432.63	202.23		This work
	298.15–730.7			125.34 + 0.078 58T/K	54
	730.7–865			−215.46 + 0.506 43T/K	
	865–913.7			202.30	This work
	913.7–960.2			208.30	
Na_2MoO_4(L)	298.15	−1412.26	223.45		This work
	298.15–730.7			125.34 + 0.078 58T/K	54
	730.7–865			−215.46 + 0.506 43T/K	
	865–913.7			202.30	This work
	913.7–960.2			208.30	
	960.2–2000			213.00	54

For Na_2MoO_4(II), based on 12 measurements between 734 and 857 K, $H_T - H_{273} = 2.532 \times 10^{-4}T^2 - 2.155 \times 10^{-1}T + 118.59$ kJ mol^{-1} (0.13%, empirical standard deviation of 0.05 kJ). This fit was assumed to be valid from 730.7 K to our selected temperature of 865 K for the II → III transition.

For Na_2MoO_4(III), based on 10 measurements between 870 and 907 K, $H_T - H_{273} = 4.456 \times 10^{-4}T^2 - 5.895 \times 10^{-1}T + 300.54$ kJ mol^{-1} (0.14%, empirical standard deviation of 0.04 kJ). This fit was assumed to be valid from 865 K to our selected temperature of 913.7 K for the III → IV transition.

A typo was detected in the article of Denielou *et al.*[54] The original constant of 30.054 kJ mol^{-1} in the fit provided for Na_2MoO_4(III) corresponded to negative values of $(H_T - H_{273})$. Adjusting this constant to 300.54 kJ mol^{-1} permitted us to reproduce (within the reported error bars) the experimental enthalpy changes of Denielou *et al.*[54] for the II → III and III → IV transitions (the two temperatures used for these calculations were those reported by the authors).

For Na_2MoO_4(IV), based on 9 measurements between 920 and 960 K, $H_T - H_{273} = -4.774 \times 10^{-4}T^2 + 1.106T + 469.86$ kJ mol^{-1} (0.16%, empirical standard deviation of 0.08 kJ). This fit was assumed to be valid from 913.7 K to our selected temperature of fusion of 960.2 K.

A marked decrease of C_P as a function of temperature was observed between the phases III and IV, owing to the mathematical expressions of $(H_T - H_{273})$ proposed by Denielou *et al.*[54] Since the temperature ranges of validity were very limited (from 870 to 907 K for III, and from 920 to 960 K for IV), the corresponding values of $(H_T - H_{273})$ were refitted by us using a linear expression (a + bT), thus leading to constant heat capacity values. Our new fits of $(H_T - H_{273})$ are $2.023 \times 10^{-1}T - 51.169$ (kJ mol^{-1}) for III, and $2.083 \times 10^{-1}T - 48.12$ (kJ mol^{-1}) for IV. The corresponding C_P values are 202.3 and 208.3 J mol^{-1} K^{-1}, respectively (see Table 17).

For $Na_2MoO_{4(L)}$, based on 14 measurements above 1091 K, $H_T - H_{273} = 2.0478 \times 10^{-1}T - 40.74$ kJ mol^{-1} (0.1%, empirical standard deviation of 0.12 kJ).

Calculated values of $H_T - H_{298}$ are shown along with the available measurements in Fig. 4. This figure includes the heat contents $H_T - H_{298}$ measured by Iyer *et al.*[92] as well as the $H_T - H_{298}$ values obtained by conversion of the $H_T - H_{273}$ data of Denielou *et al.*[54] [$H_T - H_{298} = (H_T - H_{273}) - (H_{298} - H_{273})$]. These two series of data are in good agreement.

The calculated heat capacity at low temperatures for Na_2MoO_4(I) is shown in Fig. 5 along with the measurements of Weller and King,[99] Gavrichev *et al.*,[101] and Zhidikova and Kuskov.[102]

In Fig. 4, the black full lines correspond to our final calculations while the red dashed line corresponds to heat contents $H_T - H_{298}$ obtained from the fit of the low-temperature C_P data measured by Refs. 99, 101, and 102, and shown in Fig. 5. An average deviation of about 3.7 kJ mol^{-1} is observed for the red dashed line, which is substantially higher than the error of about 0.02 kJ mol^{-1} reported by Ref. 54. This lends support to our final calculations displayed in Figs. 4 and 5.

The heat content measurements of Iyer *et al.*[92] were carried out over the temperature range 335–760 K using drop calorimetry in a high-temperature Calvet calorimeter. These authors observed transitions at 520 ± 5 and 720 ± 5 K. The first transition (at about 520 K) has not been reported previously while the DTA study of the same authors from 300 to 973 K revealed the presence of three

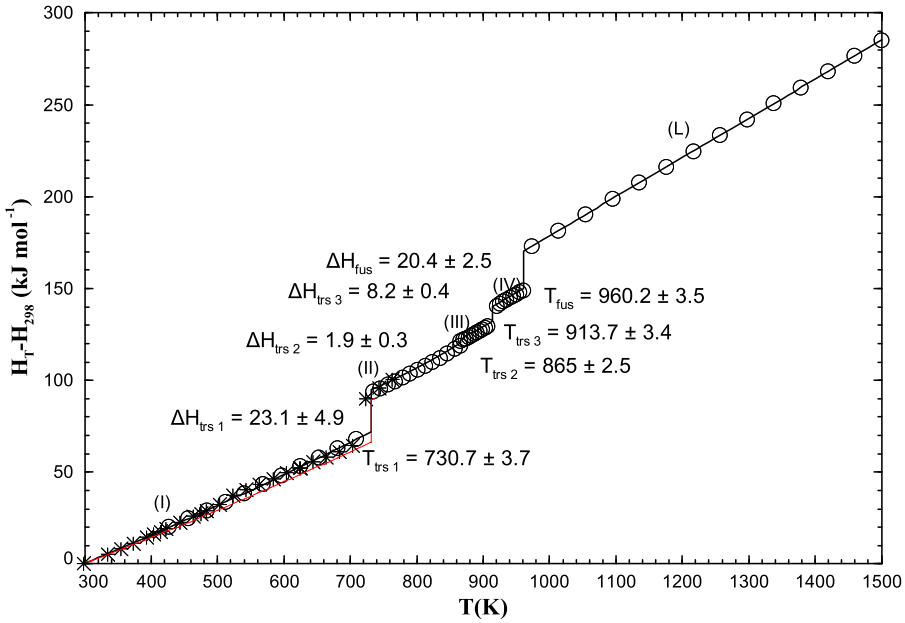

FIG. 4. Calculated heat content $H_T - H_{298}$ for Na_2MoO_4 (enthalpies of transition are the weighted average of all available data presented in Tables 13–16). Experimental data from Refs. 54 (○) and 92 (✳). Red line: $H_T - H_{298}$ fit of low-temperature heat capacity data shown in Fig. 5.

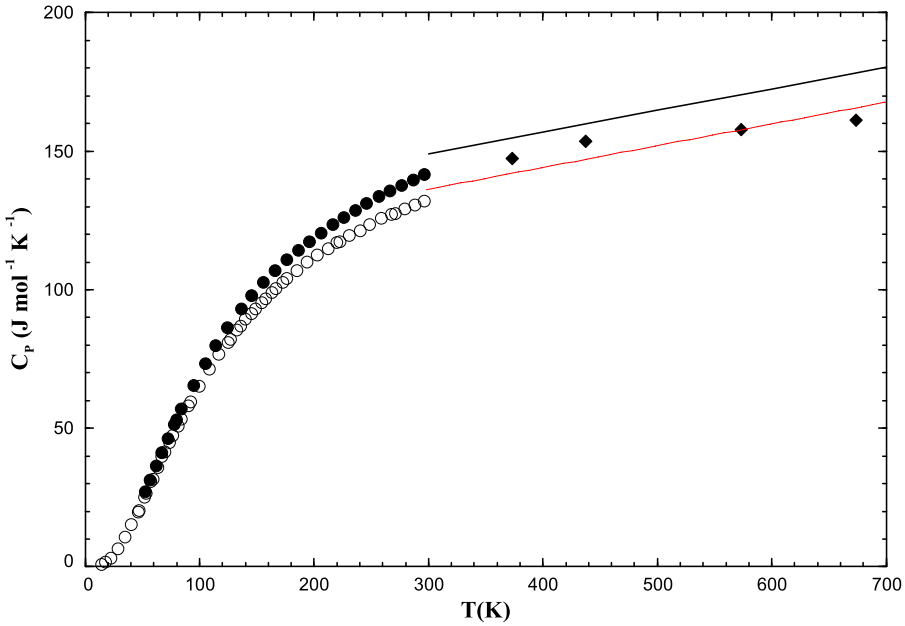

FIG. 5. Calculated heat capacity at low temperatures for Na_2MoO_4(l). Experimental data from Refs. 99 (●), 101 (○), and 102 (◆). Red line: best linear fit of C_P data above room temperature.

solid–solid transitions (at about 713, 845 and 896 K). According to Iyer *et al.*,[92] the first transition (at about 520 K) was not observed in their calorimetric study owing to the sensitivity being insufficient to detect a small enthalpy change for a small sample size. For the second transition (at about 720 K), there is good agreement between the calorimetric and DTA studies of Iyer *et al.*,[92] and also with the calorimetric measurements of Denielou *et al.*[54] using drop calorimetry in an ice calorimeter. Finally, the transition at about 520 K reported by Iyer *et al.*[92] was ignored in the present work, and only three solid–solid transitions (corresponding to the four phases I, II, III, and IV) were considered.

4.4. Potassium molybdate

4.4.1. Transition temperature (T_{trs}) and enthalpy change (ΔH_{trs}) of solid–solid transitions (I → II, II → III, and III → IV) for K_2MoO_4

The temperatures and enthalpy changes for the various solid–solid transitions (I → II, II → III, and III → IV) of K_2MoO_4 were measured by DSC in the present work. These measurements along with all data collected from the literature are displayed in Tables 18–20, respectively. Our experimental DSC thermogram is provided in the supplementary material (Fig. S3).

TABLE 18. Transition temperature and enthalpy change of transition I → II for K_2MoO_4

T_{trs} (I → II) (°C)	ΔH_{trs}(I → II) (kJ mol^{-1})	Experimental method	Reference
325.4	2.338[a]	DSC (second heating) at 10 °C/min	This work
322.2	2.236[a]	DSC (third heating) at 10 °C/min	This work
327 ± 1.5	···	Thermal study	103
323	···	Thermal analysis (cooling)	104
321	···	Thermal analysis	59
323	···	DTA	91
295.9 ± 2[a]	11.34	DTA	53
		DTA	
282.9[a]	8.27 ± 0.10	Heating 0.5 °C/min Cooling 0.42 °C/min	105
322.9 ± 1	11.34 ± 1.62	DSC (5 and 10 °C/min)	40
323.5 ± 3.8	10.6 ± 2.9	Weighted average	This work

[a]Outlier.

TABLE 19. Transition temperature and enthalpy change of transition II → III for K_2MoO_4

T_{trs} (II → III) (°C)	ΔH_{trs} (II → III) (kJ mol^{-1})	Experimental method	Reference
454.8	0.980	DSC (second heating) at 10 °C/min	This work
455.1	0.978	DSC (third heating) at 10 °C/min	This work
454 ± 1.5	···	Thermal study	103
458	···	Thermal analysis (cooling)	104
439[a]	···	Thermal analysis	59
438[a]	···	DTA	91
451.9 ± 2	1.13	DTA	53
		DTA	
456.9	0.64 ± 0.03[a]	Heating 0.5 °C/min Cooling 0.42 °C/min	105
452.9 ± 2	1.04 ± 0.06	DSC (5 and 10 °C/min)	40
454.7 ± 3.9	1.0 ± 0.1	Weighted average	This work

[a]Outlier.

TABLE 20. Transition temperature and enthalpy change of transition III → IV for K_2MoO_4

T_{trs} (III → IV) (°C)	ΔH_{trs} (III → IV) (kJ mol^{-1})	Experimental method	Reference
···	···	DSC (second heating) at 10 °C/min	This work
···	···	DSC (third heating) at 10 °C/min	This work
479.0 ± 1.5	···	Thermal study	103
480	···	Thermal analysis (cooling)	104
475	···	Thermal analysis	59
462	···	DTA	91[a]
475.9 ± 10	···	···	Reported from "V. P. Glushko (VINITI, Moscow, 1981–1982) volume 10" in Ref. 40
479.9	0.024	DSC 5 °C/min	40

[a]Another solid–solid transition at 480 °C, which was not considered in this work, has been reported by Ref. 91.

The experimental data in Tables 18–20 suggest that there are three different solid–solid transitions for K_2MoO_4. According to our high-temperature XRD measurements (at 465 and 500 °C), there are only two solid–solid transitions. Furthermore, in the second and third heating/cooling runs of our two DSC experiments, the III → IV transition was never observed. While performing DSC measurements with a heating/cooling rate of 5 K/min, Gavrichev *et al.*[40] did observe the III → IV transition and reported an extremely low enthalpy change of 0.024 kJ mol^{-1}.[40] Other studies reported a similar transition temperature[59,91,103,104] but did not measure the corresponding enthalpy change.

In most studies reporting the III → IV transition, the purity of the reagents was not indicated, and thus this transition may be due to the presence of impurities. Finally, based on our XRD and DSC measurements, only two solid–solid transitions were considered for K_2MoO_4 in the present work. Note that, if a III → IV transition were taken into account, it would have very little impact on our future calculations related to high temperature corrosion, since the corresponding enthalpy change would be very small (0.024 kJ mol^{-1}) and the phase III would be stable over a limited temperature range of less than 25 °C (i.e., between about 455 and 478 °C).

4.4.2. Temperature (T_{fus}) and enthalpy of fusion (ΔH_{fus}) for K_2MoO_4

The properties of fusion (temperature and enthalpy change) were measured by Refs. 40, 53, 59, 94–97, and 103–105.

The heat of fusion was measured by DTA,[53,105] calorimetry,[94] and DSC.[40] All experimental data from the literature and our own DSC measurements are gathered in Table 21.

4.4.3. Recommended thermodynamic data for potassium molybdate K_2MoO_4

Our selected thermodynamic data ($\Delta_f H^\circ_{298}$, S°_{298} and C_P) for potassium molybdate (K_2MoO_4) are shown in Table 22.

The standard enthalpy at 298.15 K ($\Delta_f H^\circ_{298}$) of K_2MoO_4(I) was estimated as −1497.85 kJ mol^{-1} as follows. Nelson *et al.*[65] measured by calorimetry the enthalpy of dissolution of K_2MoO_4(I) in a 10^{-3} M $OH^-_{(aq)}$ solution. These authors reported an enthalpy change of −3.97 kJ mol^{-1} for the reaction $K_2MoO_{4(I)} \rightarrow 2K^+_{(aq)} + MoO^{2-}_{4(aq)}$. According to the FactSage databases,[66] $\Delta_f H^\circ_{298}(K^+_{(aq)})$ = −251.97 kJ mol^{-1} and $\Delta_f H^\circ_{298}(MoO^{2-}_{4(aq)})$ = −997.88 kJ mol^{-1}.

TABLE 21. Transition temperature and enthalpy of fusion for K_2MoO_4

T_{fus} (III → L) (°C)	ΔH_{fus} (III → L) (kJ mol^{-1})	Experimental method	Reference
927.1	30.460[a]	DSC (second heating) at 10 °C/min	This work
927.8	28.983[a]	DSC (third heating) at 10 °C/min	This work
819 ± 1.5[a]	···	Thermal study	103
926	···	Thermal analysis (cooling)	104
936	···	Thermal analysis	59
926	···	Visual-polythermal method	95
926	···	Heating curves	96
926	38.702	DTA	53
		DTA	
925.9 ± 1	38.70	Heating at 0.5 °C/min Cooling at 0.42 °C/min	105
927.9 ± 2	34.70 ± 0.7	Calorimetry; spectroscopy	94
926	···	Thermal analysis	97
930.9 ± 1	40.14 ± 1.25	DSC (5 and 10 °C/min)	40
927.8 ± 5.9	36.6 ± 5.0	Weighted average	This work

[a]Outlier.

TABLE 22. Selected thermodynamic properties of K_2MoO_4

Phase	T range (K)	$\Delta_f H^\circ_{298}$ (kJ mol^{-1})	S°_{298} (J mol^{-1} K^{-1})	C_P (J mol^{-1} K^{-1})	Reference
K_2MoO_4(I)	298.15	−1497.85	199.30		This work 40
	298.15–596.6			113.50 + 0.096 88 T/K + 729 689.6 (T/K)$^{-2}$	This work
K_2MoO_4(II)	298.15–727.9	−1487.27	217.02	113.50 + 0.096 88 T/K + 729 689.6 (T/K)$^{-2}$	This work
K_2MoO_4(III)	298.15–730.7	−1486.26	218.42	113.50 + 0.096 88 T/K + 729 689.6 (T/K)$^{-2}$	This work
	730.7–865			−227.31 + 0.524 73 T/K + 729 689.6 (T/K)$^{-2}$	
	865–1201			196.45 + 0.018 30 T/K + 729 689.6 (T/K)$^{-2}$	
K_2MoO_4(L)	298.15–730.7	−1449.67	248.88	113.50 + 0.096 88 T/K + 729 689.6 (T/K)$^{-2}$	This work
	730.7–865			−227.31 + 0.524 73 T/K + 729 689.6 (T/K)$^{-2}$	
	865–1201			196.45 + 0.018 30 T/K + 729 689.6 (T/K)$^{-2}$	
	1201–1500			204.67 + 0.015 06 T/K	

There is no recommended value of $\Delta_f H^\circ_{298}$ for K_2MoO_4(I) in Barin's compilation tables.[67] OQMD[68,69] reported an enthalpy of formation at 0 K of −1575.70 kJ mol^{-1} using DFT. The corresponding value given in Materials Project[70] is −1493.30 kJ mol^{-1}.

The standard entropy at 298.15 K (S°_{298}) of K_2MoO_4(I) was set to the value of 199.3 J mol^{-1} K^{-1} reported by Gavrichev *et al.*[40] These authors derived this value by integration of $\int_{0K}^{298.15K} \frac{C_P}{T} dT$ using their low-temperature heat capacity data obtained by adiabatic calorimetry. To our knowledge, this is the only experimental value available in the literature. S°_{298} was estimated by us using two different exchange reactions, for which $\Delta S = 0$ was assumed at 298.15 K. We derived a value of 182.79 J mol^{-1} K^{-1} from the exchange reaction $Na_2MoO_{4(I)} + K_2CrO_{4(I)} \rightarrow K_2MoO_{4(I)} + Na_2CrO_{4(I)}$, and a value of 180.25 J mol^{-1} K^{-1} from the exchange reaction $Na_2MoO_{4(I)} + 2\,KCl_{(sol)} \rightarrow K_2MoO_{4(I)} + 2\,NaCl_{(sol)}$. The standard entropies at 298.15 K of Na_2MoO_4(I), K_2CrO_4(I) and Na_2CrO_4(I) were assessed by us in this work, and those of KCl(sol) and NaCl(sol) were taken from the FTsalt thermodynamic database.[66] Our two derived S°_{298} values are very rough estimates. These are lower than the value reported by Gavrichev *et al.*[40]

The latter value, which was selected in this work, is probably somewhat too low since the experimental S°_{298} value of Gavrichev *et al.*[101] for Na_2MoO_4 was lower by about 10 J mol^{-1} K^{-1} than the values of Refs. 67 and 99 favored in this work.

To our knowledge, the low-temperature data of Gavrichev *et al.*[40] are the only direct heat capacity measurements available for K_2MoO_4. In the present work, the heat capacity (as a function of temperature) of K_2MoO_4 was assessed from the following exchange reactions, assuming that $\Delta C_P = 0$ at all temperatures: $Na_2MoO_{4(sol)} + 2\,KCl_{(sol)} \rightarrow K_2MoO_{4(sol)} + 2\,NaCl_{(sol)}$ for the solid phases (I, II, and III), and $Na_2MoO_{4(L)} + 2\,KCl_{(L)}$

$\rightarrow K_2MoO_{4(L)} + 2\,NaCl_{(L)}$ for the pure liquid. The heat capacity of Na_2MoO_4 was evaluated in the present work, and those of KCl and NaCl were taken from the FTsalt database.[66]

In Fig. 6, the calculated heat capacity of solid K_2MoO_4 at low temperatures is compared to three series of measurements (3, 4, and 6) conducted by Gavrichev *et al.*[40] using DSC. These authors performed six different series of measurements at low temperatures: series 1 between 78.83 and 215.59 K, series 2 between 132.27 and 215.40 K, series 3 between 8.97 and 75.08 K, series 4 between 174.38 and 342.90 K, series 5 between 245 and 257.31 K, and series 6 between 99.83 and 116.16 K. Agreement from room temperature to 342.90 K (maximum temperature investigated by Gavrichev *et al.*[40]) is satisfactory.

4.5. Sodium tungstate

4.5.1. Transition temperature (T_{trs}) and enthalpy change (ΔH_{trs}) of solid–solid transitions (I → II and II → III) for Na_2WO_4

The temperatures and enthalpy changes for the solid–solid transitions (I → II and II → III) of Na_2WO_4 were measured by DSC in the present work. These measurements along with all data collected from the literature are displayed in Tables 23 and 24, respectively. Our experimental DSC thermogram is displayed in the supplementary material (Fig. S4).

4.5.2. Temperature (T_{fus}) and enthalpy of fusion (ΔH_{fus}) for Na_2WO_4

The properties of fusion (temperature and enthalpy change) were measured by Refs. 36, 46, 53, 54, 62, 86, 97, and 106–109. The heat of fusion was obtained by DTA[53,86,107,108] and drop calorimetry.[54] All experimental data collected from the literature and our own DSC measurements are compiled in Table 25.

4.5.3. Recommended thermodynamic data for sodium tungstate Na_2WO_4

Our selected thermodynamic data ($\Delta_f H^\circ_{298}$, S°_{298}, and C_P) for sodium tungstate (Na_2WO_4) are given in Table 26.

Various studies were conducted to identify the number of solid–solid transitions. Some authors reported a single solid–solid transition[33,53,54,74,108] while others reported two such transitions.[36,45,86,106,107]

Denielou *et al.*[54] used drop calorimetry to measure heat contents ($H_T - H_{273}$) whereas Riccardi and Sinistri[53] performed DTA measurements; both studies reported a single solid–solid transition (see Table 23). The DSC analyses of Bottelberghs and van Buren[36] were able to separate the peaks corresponding to the I → II and II → III transitions using a very low heating rate of 0.3 °C/min. They estimated the temperature range of stability of the phase II to be only about 2 °C. According to Bottelberghs and van Buren,[36] the previous studies did not observe the II → III transition because their calorimetric apparatuses were not calibrated with Zn, thus preventing them from measuring quantitatively and separately all solid–solid transitions.

Goranson and Kracek[107] observed large overheating and undercooling effects for the II → III transition on their differential heating and cooling curves; they reported a difference of only 1.2 °C between their temperatures for the I → II and II → III transitions. Similarly, the DSC measurements of Hämmer and Höppe[45] at a heating rate of 0.1 °C/min showed these two solid–solid transitions, with a temperature difference of only 2 °C.

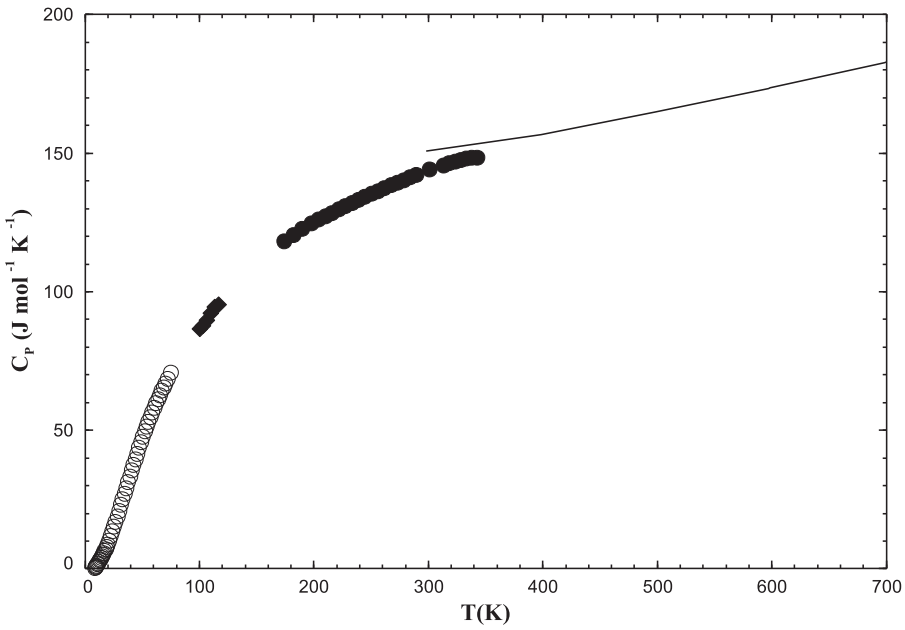

FIG. 6. Calculated heat capacity at low temperatures for K_2MoO_4(l). Experimental data from Ref. 40 (series 3 :○, series 4 :●, and series 6 :◆).

TABLE 23. Transition temperature and enthalpy change of transition I → II for Na_2WO_4

T_{trs} (I → II) (°C)	ΔH_{trs} (I → II) (kJ mol^{-1})	Experimental method	Reference
...	28.93	DSC (second heating) at 10 °C/min	This work
...	28.66	DSC (third heating) at 10 °C/min	This work
564[a]	...	Cooling curves	46
587	...	Cooling curves[b]	106
587.6	30.851	DTA	107
579[a]	39.790[a]	Heating or cooling curves	74
588	31.380 ± 0.146	DTA[c] at 1 °C/min	86
591	34.434	DTA	53
585.9 ± 3	31.506 ± 0.502	Calorimetry, drop method	54
587.9	...	DSC (cooling) at 0.3 °C/min	36
559.9[a]	...	Raman spectroscopy	33
...	3.3[a]	Thermal analysis (DSC) at 8–10 °C/min	108
589	...	DSC (heating) at 0.1 °C/min	45
588.3 ± 3.1	31.5 ± 5.9[d]	Weighted average	This work

[a]Outlier.
[b]Cooling rates were not provided, but it was mentioned that various (slow) cooling rates were used.
[c]Enthalpy changes were measured upon cooling while temperatures were measured upon heating.
[d]See explanation in text.

TABLE 24. Transition temperature and enthalpy change of transition II → III for Na_2WO_4

T_{trs} (II → III) (°C)	ΔH_{trs} (II → III) (kJ mol^{-1})	Experimental method	Reference
...	...	DSC (second heating) at 10 °C/min	This work
...	...	DSC (third heating) at 10 °C/min	This work
564–588	...	Cooling curves	46
591	...	Cooling curves[a]	106
588.8	4.113 ± 0.015	DTA	107
589	4.142 ± 0.146	DTA at 1 °C/min	86
589.9	...	DSC (cooling) at 0.3 °C/min	36
591	...	DSC (heating) at 0.1 °C/min	45

[a]Cooling rates were not provided, but it was mentioned that various (slow) cooling rates were used.

Our DSC measurements for Na_2WO_4 were performed at a heating/cooling rate of 10 °C/min. One solid–solid transition was observed upon heating whereas two different solid–solid transitions were observed upon cooling. The presence of two exothermic events in our DSC cooling curves indicates that both phase transitions were reversible.[45]

Our weighted averages of the temperatures for the I → II and II → III transitions are 588.3 and 589.6 °C (see Tables 23 and 24), respectively, with a temperature difference of only 1.3 °C. Hence, only two phases for Na_2WO_4 were considered in the present work: the low-temperature phase I and the high-temperature phase III (which was renamed II for the sake of clarity, as seen in Table 26). Nolte and Kordes,[86] and Goranson and Kracek[107] are the only authors who were able to measure the enthalpy changes of the I → II and II → III transitions. Our selected enthalpy change for the I → II transition (where the notation "II" now refers to the high-temperature phase III) is the sum of the two enthalpy changes for the I → II and II → III transitions reported in Refs. 86 and 107. (A weighted average of these two series of data was used).

For both Na_2WO_4 and Na_2MoO_4, the enthalpy change of the I → II transition is higher than the enthalpy of fusion. Therefore, for both compounds, the entropy change of the I → II transition exceeds the entropy of fusion. For Na_2WO_4, Goranson and Kracek[107] estimated the volume changes related to the I → II transition and to the fusion using their calorimetric data and the Clausius-Clapeyron relation. Based on these values (see Table 27), the molar volume change associated with the I → II transition is larger than the molar volume

TABLE 25. Transition temperature and enthalpy of fusion for Na_2WO_4

T_{fus} (III → L) (°C)	ΔH_{fus} (III → L) (kJ mol^{-1})	Experimental method	Reference
690.8	24.47	DSC (second heating) at 10 °C/min	This work
690.9	23.85	DSC (third heating) at 10 °C/min	This work
698	···	Cooling curves	46
694	···	Cooling curves	106
695.5	23.799 ± 0.015	DTA	107
698	···	Visual-polythermal analysis	109
696	31.254 ± 0.146	DTA at 1 °C/min	86
698	31.464	DTA	53
693	···	Visual-polythermal analysis	62
689	···	Thermal analysis	97
693.9 ± 2	27.865 ± 0.586	Calorimetry, drop method	54
693.9	···	DSC (cooling) at 0.3 °C/min	36
695.9 ± 2	34 ± 3.5[a]	Thermal analysis (DTA) at 8–10 °C/min	108
694.2 ± 5.6	27.0 ± 6.6	Weighted average	This work

[a]Outlier.

TABLE 26. Selected thermodynamic properties of Na_2WO_4

Phase	T range (K)	$\Delta_f H^\circ_{298}$ (kJ mol^{-1})	S°_{298} (J mol^{-1} K^{-1})	C_P (J mol^{-1} K^{-1})	Reference
Na_2WO_4(I)	298.15	−1544.73	161.08		110, 111
	298.15–861.5			130.18 + 0.067 34 T/K	54
Na_2WO_4(II)	298.15	−1513.26	197.61		This work
	298.15–861.5			130.18 + 0.067 34 T/K	54
	861.5–967.4			−29.72 + 0.255 81 T/K	
Na_2WO_4(L)	298.15	−1486.31	225.47		This work
	298.15–861.5			130.18 + 0.067 34 T/K	
	861.5–967.4			−29.72 + 0.255 81 T/K	54
	967.4–2000			216.19	

TABLE 27. Volume change of Na_2WO_4

Transition	Volume change (cm^3 g^{-1})	Volume change (cm^3 mol^{-1})	Reference
Na_2WO_4(I → II)	0.035	10.284	107
Na_2WO_4(III → L)	0.018	5.289	107

change upon melting. This explains the ranking of the corresponding entropy changes. It is very likely that the same phenomenon occurs for Na_2MoO_4.

The standard enthalpy at 298.15 K ($\Delta_f H^\circ_{298}$) of Na_2WO_4(I) was estimated by JANAF[110] from the reaction H_2WO_4(sol) + 2 NaCl(sol) = Na_2WO_4(I) + 2 HCl(aq., 12.73 H_2O), using $\Delta_f H^\circ_{298}$(H_2WO_4(sol)) = −1131.77 kJ mol^{-1} and $\Delta_f H^\circ_{298}$ (NaCl(sol)) = −411.12 kJ mol^{-1} both taken from Ref. 110, the heat of reaction $\Delta_r H^\circ_{303}$ = 81.34 ± 0.33 kJ mol^{-1} measured by Koehler *et al.*,[100] and $\Delta_f H^\circ_{298}$ ($HCl_{(aq.)}$) = −74.84 ± 62.76 kJ mol^{-1} provided in Ref. 112.

The enthalpy change at 298.15 K of the reaction W(sol) + 2 NaOH(aq) + 2 H_2O(l) = Na_2WO_4(aq) + 3 H_2(g) was measured by calorimetry as −29.29 ± 6.28 kJ mol^{-1}.[113] The heat of solution for the reaction Na_2WO_4(I) = Na_2WO_4(aq) was then measured as −7.11 ± 0.42 kJ mol^{-1}, which finally permitted to derive a value of −1541.39 kJ mol^{-1} for $\Delta_f H^\circ_{298}$ (Na_2WO_4(I)). This latter value is close to the value of −1544.73 kJ mol^{-1} recommended by JANAF.[110]

Using a cycle of calorimetric reactions, Koehler *et al.*[100] estimated $\Delta_f H^\circ_{298}$ (Na_2WO_4(I)) as −1586.57 kJ mol^{-1}.

Graham and Hepler[114] measured by calorimetry at 298.15 K the enthalpy of dissolution of Na_2WO_4(I) in small concentrations of NaOH or in 0.005–0.01 M NH_4OH, according to the reaction $Na_2WO_4(I) \rightarrow 2Na^+_{(aq)} + WO^{2-}_{4(aq)}$. From their experimental enthalpy change for the reaction H_2WO_4(sol) + 2 OH^-(aq) = WO^{2-}_4(aq) + 2 H_2O(L) and the standard enthalpies at 298.15 K of H_2WO_4(sol), OH^- and H_2O taken from Ref. 115, they first

estimated $\Delta_f H^\circ_{298}$ (WO_4^{2-} (aq)). The obtained value was consistent with that of the Bureau of Standards.[115] Then, from the latter value, the standard enthalpy at 298.15 K of $Na^+_{(aq)}$ provided by Ref. 115 and their measured enthalpy of dissolution of Na_2WO_4(I) (−6.69 ± 0.42 kJ mol^{-1}), they assessed $\Delta_f H^\circ_{298}(Na_2WO_{4(I)})$ as −1588.25 kJ mol^{-1}.

Finally, the $\Delta_f H^\circ_{298}$ value recommended by JANAF[110] was selected in this work. Indeed, according to JANAF,[110] Koehler *et al.*[100] and Graham and Hepler[114] used an erroneous value of −1172.36 kJ mol^{-1} for $\Delta_f H^\circ_{298}$ (H_2WO_4(sol)). Also, note that U.S. Nat. Bur. Stand. Circ. 500[115] reported a value of −1652.68 kJ mol^{-1} for $\Delta_f H^\circ_{298}$ (Na_2WO_4(I)). This value was derived from the experimental heat of reaction of tungsten powder using an excess of Na_2O_2. As mentioned in Ref. 110, this approach is most likely wrong owing to the possible formation of tungstate and complexes of peroxytungstate.

The standard enthalpy at 298.15 K of Na_2WO_4(I) was estimated by us using the method proposed by Hisham and Benson.[116] These authors derived equations of the type $\frac{1}{a}\Delta_f H^\circ_{298}(M_aX_b) = m\Delta_f H^\circ_{298}(MCl) + \frac{1-m}{2}\Delta_f H^\circ_{298}(M_2O) + C$, where m and C are two constants, and $\Delta_f H^\circ_{298}$ refers to the standard enthalpy at 298.15 K of the corresponding solid compound. They selected the corresponding chloride and oxide of a metal M as reference compounds since, for the majority of metals, the chloride and oxide values are known with good accuracy. For the alkali tungstates, Hisham and Benson[116] obtained m = 2.93 and C = −426.35 kJ mol^{-1}. Using the $\Delta_f H^\circ_{298}$ values for solid NaCl and Na_2O from the FactSage thermodynamic databases,[66] $\Delta_f H^\circ_{298}(Na_2WO_4$(I)) was assessed as −1554.87 kJ mol^{-1}, which is reasonably close to the value recommended by JANAF[110] and selected in the present work. OQMD[68,69] reported an enthalpy of formation at 0 K of −1637.84 kJ mol^{-1} using DFT. The corresponding value given in Materials Project[70] is −1500.06 kJ mol^{-1}.

Using calorimetry, King and Weller[111] performed low-temperature heat capacity measurements for Na_2WO_4(I), and derived from them a value of 161.08 J mol^{-1} K^{-1} for the standard entropy at 298.15 K (S°_{298}). (The temperature range from 0 to 51 K was extrapolated using the Einstein and Debye functions.) This value, which is recommended by JANAF,[110] was selected in the present work.

Na_2WO_4 was studied by Denielou *et al.*,[54] using the same experimental technique that was previously discussed in detail for Na_2CrO_4 and Na_2MoO_4. These authors provided fits (as a function of temperature) for their heat content measurements ($H_T - H_{273}$). For Na_2WO_4(I), based on 14 measurements between 345 and 849 K, $H_T - H_{273} = 3.367 \times 10^{-5}T^2 + 1.302 \times 10^{-1}T - 38.58$ kJ mol^{-1} (0.4%, empirical standard variation of 0.03 kJ). This fit was assumed to be valid from 298.15 K to our selected temperature of 861.5 K for the I → II transition.

For Na_2WO_4(II), based on 9 measurements between 862 and 957 K, $H_T - H_{273} = 1.279 \times 10^{-4}T^2 - 2.972 \times 10^{-2}T + 60.75$ kJ mol^{-1} (0.4%, empirical standard variation of 0.05 kJ). This fit was assumed to be valid from 861.5 K until our selected temperature of fusion of 967.4 K.

For Na_2WO_4(L), based on 12 measurements above 992 K, $H_T - H_{273} = 2.162 \times 10^{-1}T - 29.61$ kJ mol^{-1} (0.14%, empirical standard variation of 0.08 kJ).[54]

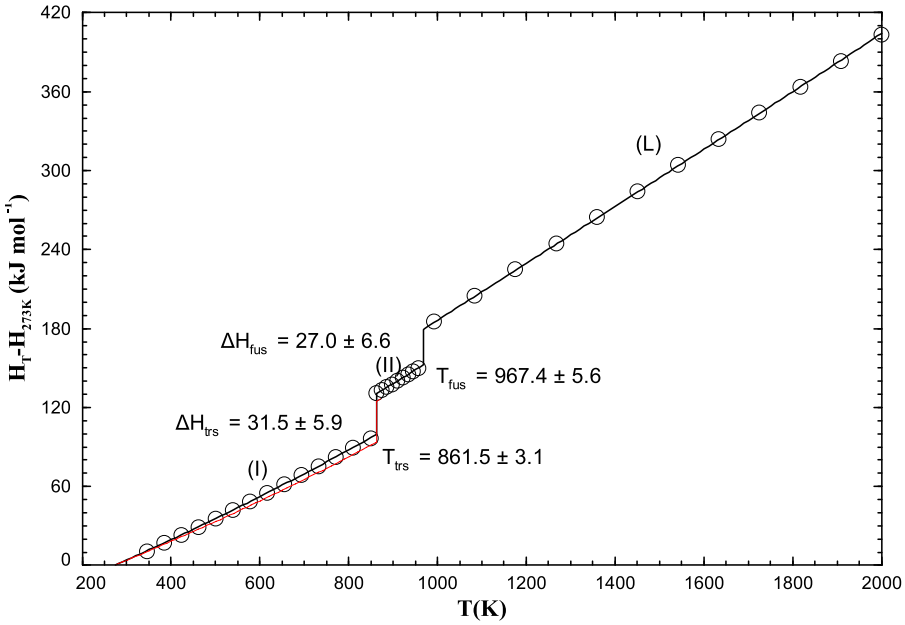

FIG. 7. Calculated heat content $H_T - H_{273}$ for Na_2WO_4 (enthalpies of transition are the weighted average of all available data presented in Tables 23 and 25). Experimental data from Ref. 54 (○). Red line: $H_T - H_{273}$ fit of low-temperature heat capacity data shown in Fig. 8.

In this work, the heat capacity expression (as a function of temperature) for Na_2WO_4 was selected in order to reproduce the heat content measurements ($H_T - H_{273}$) of Denielou *et al.*[54] Calculations are compared to the available data in Fig. 7. Also, the calculated heat capacity is shown along with the low-temperature measurements of King and Weller[111] in Fig. 8. At room temperature, agreement is reasonable.

In Fig. 7, the black full lines represent our final calculations while the red dashed line refers to $H_T - H_{273}$ heat contents obtained from the fit of the room temperature C_P data of Ref. 111 displayed in Fig. 8. An average deviation of about 4 kJ mol^{-1} is calculated for the red dashed line, which is significantly higher than the experimental error of 0.03 kJ mol^{-1} reported by Ref. 54. This lends support to our final calculations shown in Figs. 7 and 8.

4.6. Potassium tungstate

4.6.1. Transition temperature (T_{trs}) and enthalpy change (ΔH_{trs}) of solid-solid transitions (I → II and II → III) for K_2WO_4

The temperatures and enthalpy changes for the solid–solid transitions (I → II and II → III) of K_2WO_4 were measured by DSC in the present work. These measurements along with all data from the literature are shown in Tables 28 and 29, respectively. Our experimental DSC thermogram is displayed in the supplementary material (Fig. S5). Some authors reported a single solid–solid transition[86,117] while others reported two such transitions.[42,53,91,108] Our DSC measurements at a heating/cooling rate of 10 °C/min confirmed that K_2WO_4 exhibits two different solid–solid transitions.

4.6.2. Temperature (T_{fus}) and enthalpy of fusion (ΔH_{fus}) for K_2WO_4

The properties of fusion (temperature and enthalpy change) were determined by Refs. 53, 62, 73, 86, 97, 118, and 119. All experimental data from the literature and our own DSC measurements are presented in Table 30.

4.6.3. Recommended thermodynamic data for potassium tungstate K_2WO_4

Our selected thermodynamic data ($\Delta_f H^\circ_{298}$, S°_{298}, and C_P) for potassium tungstate (K_2WO_4) are given in Table 31.

The standard enthalpy at 298.15 K ($\Delta_f H^\circ_{298}$) was taken directly from the SGPS database in FactSage.[66] Indeed, this value (−1581.6 kJ mol^{-1}) is close to the value of −1574.0 kJ mol^{-1} assessed using the equation of Hisham and Benson[116] with an approach similar to that described previously for Na_2WO_4. The validity of this equation was confirmed by us for the compounds Na_2CrO_4, K_2CrO_4, Na_2MoO_4 and K_2MoO_4, for which there was good agreement between the estimated $\Delta_f H^\circ_{298}$ values and our selected values based on experimental data from the literature. For K_2WO_4, OQMD[68,69] reported an enthalpy of formation at 0 K of −1645.27 kJ mol^{-1} using DFT. The corresponding value given in Materials Project[70] is −1528.42 kJ mol^{-1}.

The standard entropy at 298.15 K (S°_{298}) of K_2WO_4(I) was taken directly from the SGPS database in FactSage[66] since no other values were available in the literature. Also, S°_{298} was roughly estimated from the exchange reactions $Na_2WO_{4(I)} + K_2CrO_{4(I)} \rightarrow K_2WO_{4(I)} + Na_2CrO_{4(I)}$ and $Na_2WO_{4(I)} + 2KCl_{(sol)} \rightarrow K_2WO_{4(I)} + 2NaCl_{(sol)}$, for which ΔS was assumed to be null at 298.15 K. The corresponding estimates are 184.46 and

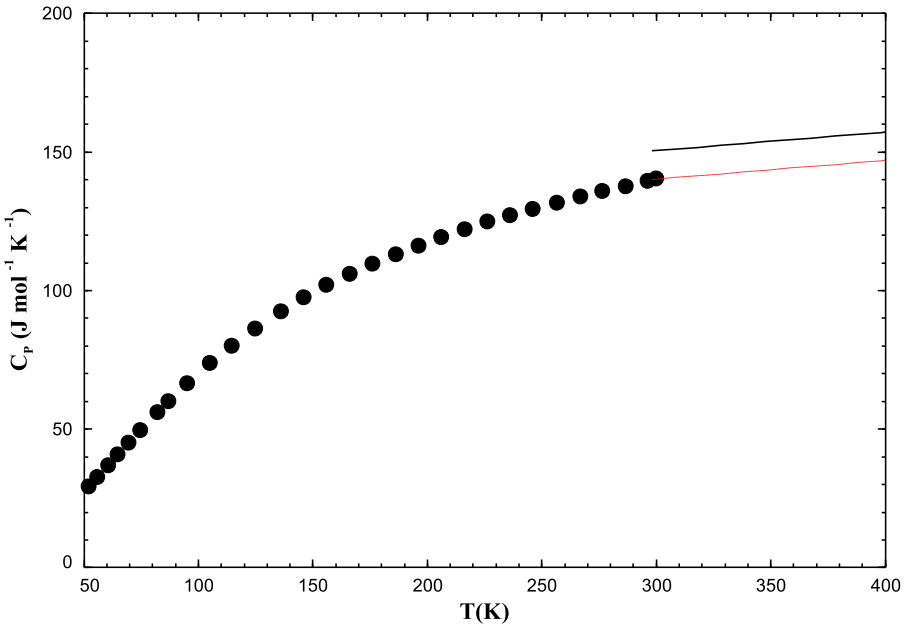

FIG. 8. Calculated heat capacity at low temperatures for Na_2WO_4(I). Experimental data from Ref. 111 (●). Red line: best linear fit of room temperature C_P data.

TABLE 28. Transition temperature and enthalpy change of transition I → II for K_2WO_4

T_{trs} (I → II) (°C)	ΔH_{trs}(I → II) (kJ mol^{-1})	Experimental method	Reference
362.7	9.82	DSC (second heating) at 10 °C/min	This work
361.7	9.84	DSC (third heating) at 10 °C/min	This work
358	···	Cooling curves	117
350[a]	9.121 ± 0.146	DTA at 1 °C/min	86
381[a]	11.464	DTA	53
370	···	DTA at 5 °C/min	91
370	···	XRD[b]	42
···	12	Thermal analysis (DTA) at 8–10 °C/min	108
364.1 ± 9.6	10.3 ± 2.2	Weighted average	This work

[a]Outlier.
[b]A high temperature focusing Guinier camera from Nonius was used with a calibrated thermocouple. The estimated error is about ±10 °C.

TABLE 29. Transition temperature and enthalpy change of transition II → III for K_2WO_4

T_{trs} (II → III) (°C)	ΔH_{trs}(II → III) (kJ mol^{-1})	Experimental method	Reference
461.1	1.031	DSC (second heating) at 10 °C/min	This work
461.3	1.001	DSC (third heating) at 10 °C/min	This work
456	1.046	DTA	53
455	···	DTA at 5 °C/min	91
435[a]	···	XRD[b]	42
···	1.2	Thermal analysis (DTA) at 8–10 °C/min	108
458.4 ± 5.7	1.1 ± 0.2	Weighted average	This work

[a]Outlier.
[b]A high temperature focusing Guinier camera from Nonius was used with a calibrated thermocouple. The estimated error is about ±10 °C.

TABLE 30. Transition temperature and enthalpy of fusion for K_2WO_4

T_{fus} (III → L) (°C)	ΔH_{fus} (III → L) (kJ mol^{-1})	Experimental method	Reference
928.2	32.47	DSC (second heating) at 10 °C/min	This work
927.7	32.57	DSC (third heating) at 10 °C/min	This work
894[a]	···	Cooling curves	73
926	···	Visual-polythermal analysis	118
926	···	Visual-polythermal analysis	119
928	31.087 ± 0.146	DTA at 1 °C/min	86
923	30.711	DTA	53
919[a]	···	Visual-polythermal analysis	62
926	···	Thermal analysis	97
926.5 ± 3.3	32.0 ± 1.7	Weighted average	This work

[a]Outlier.

TABLE 31. Selected thermodynamic properties of K_2WO_4

Phase	T range (K)	$\Delta_f H^\circ_{298}$ (kJ mol^{-1})	S°_{298} (J mol^{-1} K^{-1})	C_P (J mol^{-1} K^{-1})	Reference
K_2WO_4(I)	298.15	−1581.60	175.81		(FactSage, SGPS database[66])
	298.15–637.3			113.39 + 0.125 52 T/K	
K_2WO_4(II)	298.15	−1571.33	191.92		This work
	298.15–637.3			113.39 + 0.125 52 T/K	(FactSage, SGPS database[66])
	637.3–731.5			194.56	
K_2WO_4(III)	298.15	−1570.28	193.36		This work
	298.15–637.3			113.39 + 0.125 52 T/K	(FactSage, SGPS database[66])
	637.3–1199.6			194.56	
K_2WO_4(L)	298.15	−1538.30	220.02		This work
	298.15–637.3			113.39 + 0.125 52 T/K	
	637.3–1199.6			194.56	(FactSage, SGPS database[66])
	1199.6–2000			213.38	

TABLE 32. Summary table of recommended values

Transition	T_{trs} (°C)	$U(T_{trs})$ (°C)	ΔH_{trs} (kJ mol^{-1})	$U(\Delta H_{trs})$ (kJ mol^{-1})
Na_2CrO_4(I → II)	419.1	2.7	9.6	0.6
Na_2CrO_4(II → L)	793.3	3.2	24.3	0.9
K_2CrO_4(I → II)	669.2	7.1	7.0	0.5
K_2CrO_4(II → L)	975.9	9.9	33.1	1.8
Na_2MoO_4(I → II)	457.6	3.7	23.1	4.9
Na_2MoO_4 (II → III)	591.8	2.5	1.9	0.3
Na_2MoO_4(III → IV)	640.6	3.4	8.2	0.4
Na_2MoO_4(IV → L)	687.1	3.5	20.4	2.5
K_2MoO_4(I → II)	323.5	3.8	10.6	2.9
K_2MoO_4(II → III)	454.7	3.9	1.0	0.1
K_2MoO_4(III → L)	927.8	5.9	36.6	5.0
Na_2WO_4(I → II)	588.3	3.1	31.5	5.9
Na_2WO_4(II → L)	694.2	5.6	27.0	6.6
K_2WO_4(I → II)	364.1	9.6	10.3	2.2
K_2WO_4(II → III)	458.4	5.7	1.1	0.2
K_2WO_4(III → L)	926.5	3.3	32.0	1.7

181.92 J mol^{-1} K^{-1}, respectively, which compares reasonably well to our selected value of 175.81 J mol^{-1} K^{-1}.

To our knowledge, no experimental data for the heat capacity of K_2WO_4 are published. Therefore, the heat capacity expression (as a function of temperature) for this compound was taken directly from the SGPS database of FactSage.[66]

4.7. Summary table of recommended values

Table 32 provides a summary of all transition temperatures and enthalpies of transition estimated in the present work, along with their assessed uncertainties.

5. Conclusions

In this work, thermodynamic properties (standard enthalpy at 298.15 K, standard entropy at 298.15 K, heat capacity as a function of temperature) were selected for all condensed phases of the compounds Na_2CrO_4, K_2CrO_4, Na_2MoO_4, K_2MoO_4, Na_2WO_4 and K_2WO_4, based on a critical analysis of all available experimental data from the literature. In addition, for the six compounds, the temperatures and enthalpy changes of all solid–solid transitions and of fusion were measured by DSC. Those data were also considered for our selection of the thermodynamic properties. Crystal structures and space groups were collected from the literature for all phases of the six compounds. High-temperature XRD measurements per-

mitted us to conclude that K_2MoO_4 displays three phases instead of the four reported in several publications.

The present work is the first step towards the development of a thermodynamic model for the Na^+, $K^+//Cl^-$, SO_4^{2-}, CO_3^{2-}, CrO_4^{2-}, $Cr_2O_7^{2-}$, MoO_4^{2-}, $Mo_2O_7^{2-}$, WO_4^{2-}, $W_2O_7^{2-}$, O^{2-} system that is relevant in the high temperature corrosion of equipment such as heat-transfer tubes. A critical evaluation of the thermodynamic properties of the compounds $Na_2Cr_2O_7$, $K_2Cr_2O_7$, $Na_2Mo_2O_7$, $K_2Mo_2O_7$, $Na_2W_2O_7$ and $K_2W_2O_7$ will be described in a subsequent paper. These compounds need to be considered since reactions of the type $2\ A_2MO_4 \leftrightharpoons A_2M_2O_7 + A_2O$ (where A = Na, K and M = Cr, Mo, W) may partly occur. Through phase equilibria calculations (which will avoid a tedious and costly trial and error experimental approach), the developed thermodynamic model will permit us to better understand high temperature corrosion phenomena in the temperature range 600–950 °C. The developed thermodynamic model will also enable a better investigation of the chemistry of ash deposits and heat exchanger alloys since the combined ash/gas/alloy chemistry controls the melting behaviour of ashes.

Supplementary Material

See the supplementary material for DSC thermograms and scatter plots for Na_2CrO_4, K_2CrO_4, Na_2MoO_4, K_2MoO_4, Na_2WO_4, and K_2WO_4.

Acknowledgments

Ms. Sara Benalia would like to thank the Canada Research Chair in Computational Thermodynamics for High Temperature Sustainable Processes held by Professor Patrice Chartrand and the Johan Gadolin Process Chemistry Centre for the 5 month-mobility grant awarded for her stay at Åbo Akademi University (Turku, Finland). The authors would like to thank Mr. Peter Backman and Ms. Jaana Paananen for operating the DSC apparatus, Ms. Evguenia Sokolenko for helping locate old articles and for translating them into English, Dr. Paul Lafaye for fruitful discussions, and Mr. Maxime Aubé for his helpful comments on the manuscript.

7. Author Declarations

7.1. Conflict of interest

The authors have no conflict to disclose.

8. Data Availability

The data that support the findings of this study are available within the article and its supplementary material.

9. References

[1] L. Antoni and A. Galerie, "Corrosion sèche des métaux. Cas industriels: Dépôts, milieux fondus," in Techniques de l'ingénieur. Matériaux métalliques, 2003.
[2] B. J. Skrifvars, R. Backman, M. Hupa, K. Salmenoja, and E. Vakkilainen, Corros. Sci. **50**, 1274–1282 (2008).
[3] L. L. Baxter, T. R. Miles, T. R. Miles, B. M. Jenkins, T. Milne, D. Dayton, R. W. Bryers, and L. L. Oden, Fuel Process. Technol. **54**, 47–78 (1998).
[4] H. P. Nielsen, F. J. Frandsen, K. Dam-Johansen, and L. L. Baxter, Prog. Energy Combust. Sci. **26**, 283–298 (2000).
[5] J. Stringer, Mater. Sci. Technol. **3**, 482–493 (1987).
[6] N. Eliaz, G. Shemesh, and R. Latanision, Eng. Failure Anal. **9**, 31–43 (2002).
[7] H. J. Grabke, E. Reese, and M. Spiegel, Corros. Sci. **37**, 1023–1043 (1995).
[8] A.-M. Huntz and B. Pieraggi, *Oxydation des Matériaux Métalliques: Comportement à Haute Température* (Hermes-Lavoisier, Paris, 2003).
[9] G. Béranger, J. C. Colson, and F. Dabosi, *Corrosion des Matériaux à Haute Température* (Editions de Physique, Les Ulis, France, 1987).
[10] J. A. Goebel, F. S. Pettit, and G. W. Goward, Metall. Trans. **4**, 261–278 (1973).
[11] A. K. Misra and C. A. Stearns, Report No. 0499-9320, NASA Lewis Research Center, Cleveland, OH, 1983.
[12] A. K. Misra, J. Electrochem. Soc. **133**, 1029–1038 (1986).
[13] M. Paneru, G. Stein-Brzozowska, J. Maier, and G. Scheffknecht, Energy Fuels **27**, 5699–5705 (2013).
[14] J. Lehmusto, D. Lindberg, P. Yrjas, B.-J. Skrifvars, and M. Hupa, Oxid. Met. **77**, 129–148 (2012).
[15] G. Fryburg, F. Kohl, and C. Stearns, J. Electrochem. Soc. **131**, 2985–2997 (1984).
[16] G. C. Fryburg, F. J. Kohl, C. A. Stearns, and W. L. Fielder, J. Electrochem. Soc. **129**, 571–585 (1982).
[17] Z. Foroulis and W. Smeltzer, *Metal-Slag-Gas Reactions and Processes* (Electrothermics, Metallurgy, and Corrosion Divisions, Princeton University, Princeton, NJ, 1975).
[18] Y. Bourhis and C. Saint-John, Proc. Electrochem. Soc. **77-1**, 595–606 (1976).
[19] S. Benalia, C. Robelin, and P. Chartrand, paper presented at the REWAS 2022: Energy Technologies and CO_2 Management (Volume II), Cham, 2022.
[20] J. J. Miller, Z. Kristallogr. - Cryst. Mater. **94**, 131–136 (1936).
[21] H. Fischmeister, Acta Crystallogr. **7**, 776–777 (1954).
[22] A. Niggli, Acta Crystallogr. **7**, 776 (1954).
[23] A. Goldberg, W. Eysel, and T. Hahn, Neues Jahrb. Mineral., Monatsh. **6**, 241–252 (1973).
[24] J. Nimmo, Acta Crystallogr., Sect. B: Struct. Crystallogr. Cryst. Chem. **37**, 431–433 (1981).
[25] V. Amirthalingam and K. S. Venkateswarlu, Thermochim. Acta **58**, 107–109 (1982).
[26] M. J. Ferrante, J. Stuve, G. Daut, and L. Pankratz, *Final Report of Investigations* (Albany Metallurgy Research Center, Bureau of Mines, Albany, OR, 1978).
[27] C. W. Pistorius, Z. Phys. Chem. **35**, 109–121 (1962).
[28] J. A. McGinnety, Acta Crystallogr., Sect. B: Struct. Crystallogr. Cryst. Chem. **28**, 2845–2852 (1972).
[29] W. Eysel, Am. Mineral. **58**, 736–747 (1973).
[30] I. Lindqvist *et al.*, Acta Chem. Scand. **4**, 1066–1074 (1950).
[31] H. E. Swanson, *Standard X-Ray Diffraction Powder Patterns: Data for 46 Substances* (National Bureau of Standards, Washington, DC, 1962).
[32] K. D. Singh Mudher, M. Keskar, K. Krishnan, and V. Venugopal, J. Alloys Compd. **396**, 275–279 (2005).
[33] C. L. Lima, G. Saraiva, P. Freire, M. Maczka, W. Paraguassu, F. De Sousa, and J. Mendes Filho, J. Raman Spectrosc. **42**, 799–802 (2011).
[34] K. Bramnik and H. Ehrenberg, Z. Anorg. Allg. Chem. **630**, 1336–1341 (2004).
[35] A. D. Fortes, Acta Crystallogr., Sect. E: Crystallogr. Commun. **71**, 592–596 (2015).
[36] P. H. Bottelberghs and F. R. van Buren, J. Solid State Chem. **13**, 182–191 (1975).
[37] B. Gatehouse and P. Leverett, J. Chem. Soc. A **1969**, 849–854.
[38] F. Kools, A. Koster, and G. Rieck, Acta Crystallogr., Sect. B: Struct. Crystallogr. Cryst. Chem. **26**, 1974–1977 (1970).
[39] J. Warczewski, Phase Transitions **1**, 131–142 (1979).
[40] K. S. Gavrichev, M. A. Ryumin, A. V. Tyurin, V. M. Gurevich, L. N. Komissarova, A. V. Khoroshilov, and G. A. Sharpataya, Russ. J. Phys. Chem. A **83**, 327–333 (2009).
[41] A. Van Den Berg, H. Overeijnder, and F. Tuinstra, Acta Crystallogr., Sect. C **39**, 678–680 (1983).
[42] A. Van Den Akker, A. Koster, and G. Rieck, J. Appl. Crystallogr. **3**, 389–392 (1970).
[43] C. W. Pistorius, J. Chem. Phys. **44**, 4532–4537 (1966).
[44] K. Okada, H. Morikawa, F. Marumo, and S. Iwai, Acta Crystallogr., Sect. B: Struct. Crystallogr. Cryst. Chem. **30**, 1872–1873 (1974).

[45]M. Hämmer and H. A. Höppe, Z. Anorg. Allg. Chem. **648**, e202100373 (2022).
[46]H. E. Boeke, Z. Anorg. Chem. **50**, 355 (1906).
[47]J. B. Austin and R. H. H. Pierce, J. Chem. Phys. **3**, 683–686 (1935).
[48]J. Wang, J. You, M. Wang, L. Lu, A. A. Sobol, and S. Wan, J. Raman Spectrosc. **49**, 1693–1705 (2018).
[49]K. Okada, H. Morikawa, F. Marumo, and S. Iwai, Acta Crystallogr., Sect. B: Struct. Crystallogr. Cryst. Chem. **31**, 1200–1201 (1975).
[50]C. Luz-Lima, J. C. Batista, P. T. C. Freire, G. P. de Sousa, F. E. P. dos Santos, J. Mendes Filho, B. C. Viana, and G. D. Saraiva, Vib. Spectrosc. **65**, 58–65 (2013).
[51]E. Flach, *Kaliumchromat und Natriumchromat, ihre Fähigkeit zur Mischkristall- und Doppelsalz-Bildung und ihre Beziehungen zu den Entsprechenden Sulfaten* (Gressner & Schramm, Leipzig, 1912), Vol. 37.
[52]C. W. Pistorius, J. Chem. Phys. **43**, 2895–2898 (1965).
[53]R. Riccardi and C. Sinistri, Ric. Sci. Parte 2 Rend. Sez. A: Abiol. **8**, 1026–1037 (1965).
[54]L. Denielou, Y. Fournier, J. Petitet, and C. Tequi, C. R. Acad. Sci. Paris, Sér. C **272**, 1855–1857 (1971).
[55]L. Doyen and R. Frech, J. Chem. Phys. **104**, 7847–7853 (1996).
[56]I. S. Rasonskaya and A. G. Bergman, Dokl. Akad. Nauk SSSR **38**, 176–180 (1943).
[57]Y. Vilnyanski and O. Pudovkina, J. Appl. Chem. USSR **20**, 794 (1947).
[58]W. H. Hartford, Ind. Eng. Chem. **41**, 1993–1997 (1949).
[59]O. Schmitz-Dumont and A. Weeg, Z. Anorg. Allg. Chem. **265**, 139–155 (1951).
[60]Z. A. Mateiko and G. A. Bukhalova, Zh. Neorg. Khim. **4**, 2329–2334 (1959).
[61]A. Stingele, "Melting point and phase diagram determination with a new precision high-temperature microscope technique," in *Thermodynamics of Nuclear Materials*, 1967 (International Atomic Energy Agency, Vienna, 1968).
[62]A. G. Bergman and A. S. Sanzharov, Ukr. Chem. J. **35**, 1328 (1969).
[63]Y. Shinata, Oxid. Met. **27**, 315–332 (1987).
[64]V. Tathavadkar, M. Antony, and A. Jha, paper presented at the Light Metals Proceedings (AIME, Warrendale, PA, 2002).
[65]T. Nelson, C. Moss, and L. G. Hepler, J. Phys. Chem. **64**, 376–377 (1960).
[66]C. W. Bale, E. Bélisle, P. Chartrand, S. A. Decterov, G. Eriksson, A. E. Gheribi, K. Hack, I. H. Jung, Y. B. Kang, J. Melançon, A. D. Pelton, S. Petersen, C. Robelin, J. Sangster, P. Spencer, and M. A. Van Ende, Calphad **54**, 35–53 (2016).
[67]I. Barin, *Thermochemical Data of Pure Substances* (VCH, Weinheim, 1989).
[68]J. E. Saal, S. Kirklin, M. Aykol, B. Meredig, and C. Wolverton, JOM **65**, 1501–1509 (2013).
[69]S. Kirklin, J. E. Saal, B. Meredig, A. Thompson, J. W. Doak, M. Aykol, S. Rühl, and C. Wolverton, npj Comput. Mater. **1**, 15010 (2015).
[70]A. Jain, S. P. Ong, G. Hautier, W. Chen, W. D. Richards, S. Dacek, S. Cholia, D. Gunter, D. Skinner, G. Ceder, and K. A. Persson, APL Mater. **1**, 011002 (2013).
[71]E. Groschuff, Z. Anorg. Chem. **58**, 102–112 (1908).
[72]S. Żemczużny, Z. Anorg. Allg. Chem. **57**, 267–277 (1908).
[73]M. Amadori, Atti Accad. Naz. Lincei, Cl. Sci. Fis., Mat. Nat. **22**, 609–616 (1913).
[74]B. Hare, London, Edinburgh, Dublin Philos. Mag. J. Sci. **48**, 412–421 (1924).
[75]D. F. Smith and F. A. Hartgen, Bureau of Mines Report of Investigations No. 2917, 1929, pp. 1–3.
[76]E. P. Dergunov and A. G. Bergman, Izvest. Sektora Fiz.-Khim. Anal., Inst. Obshcheĭ Neorg. Khim., Akad. Nauk S.S.S.R **21**, 184–198 (1952).
[77]E. Lax, *Taschenbuch für Chemiker und Physiker-Band 1: Makroskopische Physikalisch-Chemische Eigenschaften* (Springer, Berlin, 1967).
[78]C. W. F. T. Pistorius and E. Rapoport, J. Phys. Chem. Solids **30**, 195–201 (1969).
[79]M. Natarajan and E. A. Secco, Can. J. Chem. **52**, 2436–2438 (1974).
[80]D. Sirousse-Zia, Thermochim. Acta **19**, 244–246 (1977).
[81]K. Kostyrko, M. Skoczylas, and A. Klee, J. Therm. Anal. **33**, 351–357 (1988).
[82]G. Janz and J. Slowick, Z. Anorg. Allg. Chem. **586**, 166–174 (1990).
[83]B.-K. Choi, J. Phys.: Condens. Matter **11**, 713 (1999).
[84]J. W. Mellor, *A Comprehensive Treatise on Inorganic and Theoretical Chemistry. Vol. XI. Te, Cr, Mo, W* (Longmans, Green & Co, Great Britain, 1931).
[85]A. G. Bergman and O. R. Vartbaronov, Zh. Neorg. Khim. **2**, 2641–2648 (1957).
[86]G. Nolte and E. Kordes, Z. Anorg. Allg. Chem. **371**, 149–155 (1969).
[87]A. G. Bergman and A. S. Sanzharov, Zh. Neorg. Khim. **14**, 2588–2589 (1969).
[88]G. A. Bukhalova and Z. N. Topshino, Zh. Neorg. Khim. **18**, 1375–1378 (1973).
[89]D. D. Wagman, W. H. Evans, V. B. Parker, R. H. Schumm, I. Halow, S. M. Bailey, K. L. Churney, and R. L. Nuttall, J. Phys. Chem. Ref. Data **18**, 1807–1812 (1989).
[90]M. M. Popov and V. P. Kolesov, Zh. Obshch. Khim. **26**, 2385–2393 (1956).
[91]P. Caillet, Bull. Soc. Chim. Fr. **12**, 4750–4755 (1967).
[92]V. S. Iyer, R. Agarwal, K. N. Roy, S. Venkateswaran, V. Venugopal, and D. D. Sood, J. Chem. Thermodyn. **22**, 439–448 (1990).
[93]A. V. Khoroshilov, G. A. Sharpataya, K. S. Gavrichev, and M. A. Ryumin, Russ. J. Inorg. Chem. **57**, 1123–1127 (2012).
[94]S. Julsrud and O. J. Kleppa, Acta Chem. Scand. **35a**, 669–678 (1981).
[95]G. A. Bukhalova and Z. A. Mateiko, Zh. Obshch. Khim. **25**, 851–857 (1955).
[96]I. N. Belyaev, Zh. Neorg. Khim. **6**, 1178–1188 (1961).
[97]G. K. Shurdumov, Z. L. Khakulov, M. V. Mokhosoev, Kh. A. Kodzokov, and R. M. El'mesova, Zh. Neorg. Khim. **29**, 2096–2101 (1984).
[98]R. P. Tangri, V. Venugopal, and D. K. Bose, Thermochim. Acta **198**, 259–265 (1992).
[99]W. W. Weller and E. G. King, Bureau of Mines Report of Investigations No. 6147, U.S. Dept. of the Interior library, Washington, DC, 1963, p. 6.
[100]M. F. Koehler, L. B. Pankratz, and R. Barany, Bureau of Mines Report of Investigations No. 5973, U.S. Dept. of the Interior library, Washington, DC, 1962, p. 13.
[101]K. S. Gavrichev, N. N. Smirnova, M. A. Ryumin, A. V. Tyurin, V. M. Gurevich, and L. N. Komissarova, Thermochim. Acta **463**, 41–43 (2007).
[102]A. P. Zhidikova and O. L. Kuskov, Geokhimiya **9**, 1149–1151 (1971).
[103]H. S. Klooster, Z. Anorg. Chem. **85**, 49–64 (1914).
[104]F. Hoermann, Z. Anorg. Allg. Chem. **177**, 145–186 (1929).
[105]H. Isozaki and T. Ozawa, Bull. Chem. Soc. Jpn. **39**, 2307–2308 (1966).
[106]F. Jaeger and H. Van Klooster, Proc. K. Ned. Akad. Wet., Ser. B: Phys. Sci. **16**, 857–880 (1914).
[107]R. Goranson and F. Kracek, J. Chem. Phys. **3**, 87–92 (1935).
[108]Y. L. Suponitskiy, E. S. Zolotova, A. G. Dyunin, and S. E. Liashenko, Russ. J. Phys. Chem. A **92**, 397–400 (2018).
[109]G. A. Bukhalova and Z. A. Mateiko, Zh. Obshch. Khim. **26**, 2119–2124 (1956).
[110]M. W. Chase, Jr., J. Phys. Chem. Ref. Data, Monograph **9**, 1–1951 (1998).
[111]E. G. King and W. W. Weller, *Low-Temperature Heat Capacities and Entropies at 298.150 K of Monotungstates of Sodium, Magnesium, and Calcium* (U.S. Department of the Interior, Bureau of Mines, Washington, DC, 1961).
[112]V. B. Parker, *Thermal Properties of Aqueous Uni-Univalent Electrolytes* (U.S. Government Printing Office, Washington, DC, 1965).
[113]J. Sherfey and A. Brenner, J. Electrochem. Soc. **105**, 665 (1958).
[114]R. L. Graham and L. G. Hepler, J. Am. Chem. Soc. **80**, 3538–3540 (1958).
[115]F. D. Rossini, W. H. Evans, S. Levine, and I. Jaffe, *Circular of the Bureau of Standards No. 500: Selected Values of Chemical Thermodynamic Properties* (U.S. Department of Commerce, National Institute of Standards and Technology, Washington, DC, 1952).
[116]M. W. Hisham and S. W. Benson, J. Phys. Chem. **92**, 6107–6112 (1988).
[117]J. A. M. van Liempt, Z. Anorg. Allg. Chem. **122**, 175 (1922).
[118]A. G. Bergman, A. I. Kislova, and V. L. Posypaiko, Zh. Obshch. Khim. **25**, 9–11 (1955).
[119]G. A. Bukhalova and Z. A. Mateiko, Zh. Obshch. Khim. **26**, 2365–2370 (1956).